A genome-wide CRISPR screen unveils the endosomal maturation protein WDR91 as a promoter of productive ASO activity in melanoma

Grégory Menchon, Aris Gaci, Antti Matvere, Marc Aubry, Aurélien Bore, David Gilot, Aurelie Goyenvalle, Rémy Pedeux

Molecular Therapy
Nucleic Acids
Original Article

A genome-wide CRISPR screen unveils the endosomal maturation protein WDR91 as a promoter of productive ASO activity in melanoma

Grégory Menchon,[1] Aris Gaci,[2] Antti Matvere,[1] Marc Aubry,[1] Aurélien Bore,[3] David Gilot,[1,4] Aurélie Goyenvalle,[2] and Rémy Pedeux[1]

[1]Univ Rennes, INSERM, OSS (Oncogenesis Stress Signaling), UMR_S 1242, CLCC Eugene Marquis, F-35000, Rennes, France; [2]Université Paris-Saclay, UVSQ, Inserm, END-ICAP, 78000 Versailles, France; [3]CRISPR'iT Genetic Platform Screening, Institut Curie, INSERM U934, CNRS UMR3215, 75005 Paris, France; [4]Assays, Profiling & Cell Sciences, Discovery Sciences, R&D, AstraZeneca, 48183 Gothenburg, Sweden

Antisense oligonucleotides (ASOs) belong to promising therapeutics for the treatment of neurological, muscular, and metabolic disorders. Several ASOs have been approved so far and more than 100 clinical trials are currently underway covering a dozen therapeutic areas. Yet, the mechanisms of internalization and cell trafficking of these molecules remain poorly understood. Moreover, with only a small fraction of ASOs reaching the correct cellular compartment after systemic delivery, the majority of targeted diseases require recurrent injections of ASOs. A deeper understanding of these mechanisms would guide the improvement of their potency and, thus, reduce the amount of delivered ASOs and their potential side effects. Here, using a CRISPR screen, we investigated intracellular proteins involved in ASOs efficiency using a whole genome approach and identified several potential regulators that could significantly impact ASOs potency in melanoma cells. We validated WD repeat domain 91, a regulator of endosomal maturation, as a modulator whose depletion significantly inhibits ASO productive activity. This study provides a list of ASO modulators using a biologically relevant assay to estimate the role of these proteins. In conclusion, these data could lead to a better understanding of the mechanisms favoring productive uptake or improved endosomal escape of ASOs.

INTRODUCTION

Antisense oligonucleotides (ASOs) belong to a class of attractive therapeutic compounds for numerous diseases. ASOs modulate cellular target gene expression through Watson-Crick binding to complementary RNA molecules and, according to their type, act by either promoting a RNAse-H1 mediated RNA degradation (Gapmers [GMs]) or through a steric blocking mechanism (mixmers and target site blockers [TSBs]) leading to three major modes of action: inhibition or activation of gene expression and splicing modulation.[1] ASOs have been developed for the treatment of different genetic disorders and they can be translated to personalized therapies.[2] ASOs are specially taken up by fast growing cells[3] and, among numerous advantages, bypass the current bottleneck regarding the targets that are considered undruggable with traditional small molecule inhibitors.[4] Several ASOs are currently approved by the U.S. Food and Drug Administration for genetic and rare diseases[5,6] and several phase II and III studies are ongoing in the oncology therapeutic area.[7]

Although ASOs promise a great leap forward in future cancer treatments, their use suffers from major hurdles. Among these hurdles, a lack of tissue-specific targeting,[8,9] the poor cellular uptake,[10] and the need to escape from the endo-lysosomal pathway to exert their role in either the cytoplasm or nucleus of the cells are of main concerns.[11,12] Moreover, the mechanisms of internalization, cell trafficking, and action of these molecules remain poorly understood. A small fraction of ASOs reaching the right cellular compartment and target after systemic delivery[13,14] leads to treatments consisting of high doses, recurrent injections, and, thus, significant accumulation in other non-targeted cells and organs with consecutive toxicities.[15] It is, therefore, essential to better understand the fate of internalized ASOs and their intracellular route and mode of action. Such deeper characterization in different cell lines and with different ASO types and chemistries would help in the rational design and improvement of therapeutic ASO strategies in future clinical applications. Several studies have demonstrated that the fate of internalized phosphorothioate (PS)-containing ASOs was determined by intracellular interacting proteins.[16–18] Even if a clear mechanism is still to be fully understood, approximately 80 intracellular proteins have been identified and this protein interactome seems to influence the pharmacological activities and potential toxicities of PS-ASOs by acting on their uptake and distribution. It is also worth noting that many other

Received 7 October 2024; accepted 21 May 2025;
https://doi.org/10.1016/j.omtn.2025.102577.

Correspondence: Aurélie Goyenvalle, Université Paris-Saclay, UVSQ, Inserm, END-ICAP, 78000 Versailles, France.
E-mail: aurelie.goyenvalle@uvsq.fr
Correspondence: Rémy Pedeux, INSERM, OSS, UMR_S 1242, University Rennes, 35000 Rennes, France.
E-mail: remy.pedeux@univ-rennes.fr

proteins that bind to ASOs have no effect on their activity. PS-ASOs are internalized and processed through the endocytic pathway,[3,19] but proteins can modulate endosome traffic and maturation without interacting directly with oligonucleotides. Previous studies have investigated the modulation of intracellular pathways to increase the productive delivery and activity of oligonucleotides and to further unveil the critical molecular factors that contribute to nucleic acids pharmacological effects.[20] Among these, modulation of endocytic recycling,[21,22] multivesicular bodies' (MVBs) fusion with lysosomes,[23] endosomal escape,[24] and nuclear shuttling[25,26] were explored. All these strategies involve the use of either genetic or non-genetic perturbations and have proven to be successful in many *in vitro* and *in vivo* studies. ASO-interacting proteins have been mostly characterized by *in vitro* studies using pull-down experiments on cell lysates,[16,17] but such methods lack physiological relevance as the intracellular membrane's integrity is not preserved and could lead to many binding artifacts. Furthermore, pull-down studies may highlight some important ASOs protein modulators but only allow the identification of direct interactants. To circumvent these issues other authors recently used proximity biotinylation assay to highlight oligonucleotides interactome in living cells and in pharmacologically relevant conditions.[27]

The CRISPR screen is a powerful genetic perturbation method that can be used for functional genomic studies, by activating or silencing genes.[28] Then, it can be implemented to identify ASOs' direct and indirect modulators in a more physiological state and preserving the cell membrane's integrity. This technique was implemented in different studies to investigate modulators of dsRNAs,[29] antibody-drug conjugates[30] or encapsulated mRNAs,[31] but to our knowledge, only one study describes such a functional genomic screen (CRISPR gene activation) to uncover factors enhancing ASOs activity.[32]

In the present work, we used a genome-wide CRISPR screen strategy (CRISPR knockout), to uncover proteins that modulate the potency of an anti-proliferative tricyclo-DNA (tcDNA) based-ASO in a melanoma cell line (501Mel). The generation of the parental knockout cell library was performed such that every single cell had a unique depleted coding gene. The library was then treated with ASOs, and sequencing was performed on the surviving (enriched or depleted) cells. This analysis highlighted several candidates of interest (95 activators and 55 inhibitors). From the top candidates, the robustness of our assay also allowed to highlight the proteins Ras-related protein RAB5C and component of oligomeric Golgi complex 8 (COG8) which are known positive regulators of ASOs productive trafficking and activity.[29,33] We unveiled the endosomal maturation protein WD repeat domain 91 (WDR91) as a strong positive regulator of the tcDNA based-ASO activity in this cell line. Activity modulation by WDR91 was validated together with Annexin A2 (ANXA2), a well-characterized endosomal protein that promotes ASOs trafficking and productive activity in different cell lines.[34] The impact of WDR91 was validated using two different ASO chemistries, but was not validated on a splice-switching ASO in a muscle cell line, highlighting a cell-type-dependent effect. Finally, this work provides a detailed source of potential positive and negative regulators of ASO activity, coming from an unbiased screen and with a strong physiological relevance.

RESULTS

Development and *in vitro* validation of a tcDNA-ASO to inhibit 501Mel cells proliferation with a target-site blocking mechanism

Previous work aiming at masking a microRNA (miRNA) target site on a miRNA sponge (*TYRP1* mRNA) led to the test and validation of a commercially designed locked nucleic acid (LNA) TSB (named TSB-T3 for target-site blocking). In this study, TSB-T3 significantly induced the reduction of melanoma tumor growth *in vitro* and in 501Mel xenografts.[35] This ASO was validated in five different cell lines and had a dose-response anti-proliferative activity. TSB-T3 exerts its ASO-masking activity by preventing the sequestration of the miR-16 tumor suppressor by *TYRP1* mRNA and redirecting it toward its target-RNAs, to induce their decay and subsequently reduce tumor proliferation (Figure 1A).[36] This miRNA displacement mediated by a TSB ASO represents a relevant assay to investigate the proteins involved in ASOs efficiency. The ASO-blocking activity is directly monitored through an anti-proliferative effect, which has been validated *in vivo*.

In the present study, we decided to look for protein modulators of an ASO with a clinically relevant chemistry. We thus designed and evaluated a new TSB-T3 with the same sequence but with a full tcDNA chemistry and PS backbone (tcT3). This class of conformationally constrained ASO displays enhanced binding properties to DNA and RNA as well as unique pharmacological properties and unprecedented uptake by many tissues after systemic administration.[37,38]

To compare both chemistries, 501Mel cells were reverse transfected in 96-well plates with either the LNA or the tcDNA ASO (named, respectively, T3 and tcT3). We deliberately used high doses of ASOs (up to 70 nM), as their blocking activity is based on the displacement of a sequestered miR-16 by *TYRP1* mRNA that is, besides, highly expressed in melanoma cells (with approximately 3,200 copies per cell).[35] After 72 h, the cell density was measured by colorimetric assay and normalized to a control ASO treatment (C1 or tcC1). As expected, we confirmed previous results with the commercial reagent. Both T3 and tcT3 ASOs showed a dose-response anti-proliferative activity and, interestingly, the tcDNA chemistry improved the ASO potency at low doses (Figure 1B). This tcDNA-ASO was selected for the subsequent screening experiment.

Genome-wide pooled single guide RNA library generation, knockout library treatment with tcDNA-ASOs, and NGS sequencing

The CRISPR-knockout cell library was generated by transducing 501Mel cells with a pooled lentiviral library which contains the Cas9 and single guide RNAs (sgRNAs) targeting 19,114 human coding genes. This lentivirus library contains an average of 4 different guides per coding gene (total of 76,441 sgRNAs) and 1,000 non-targeting control sgRNAs. A multiplicity of infection (MOI) of 0.4 was selected

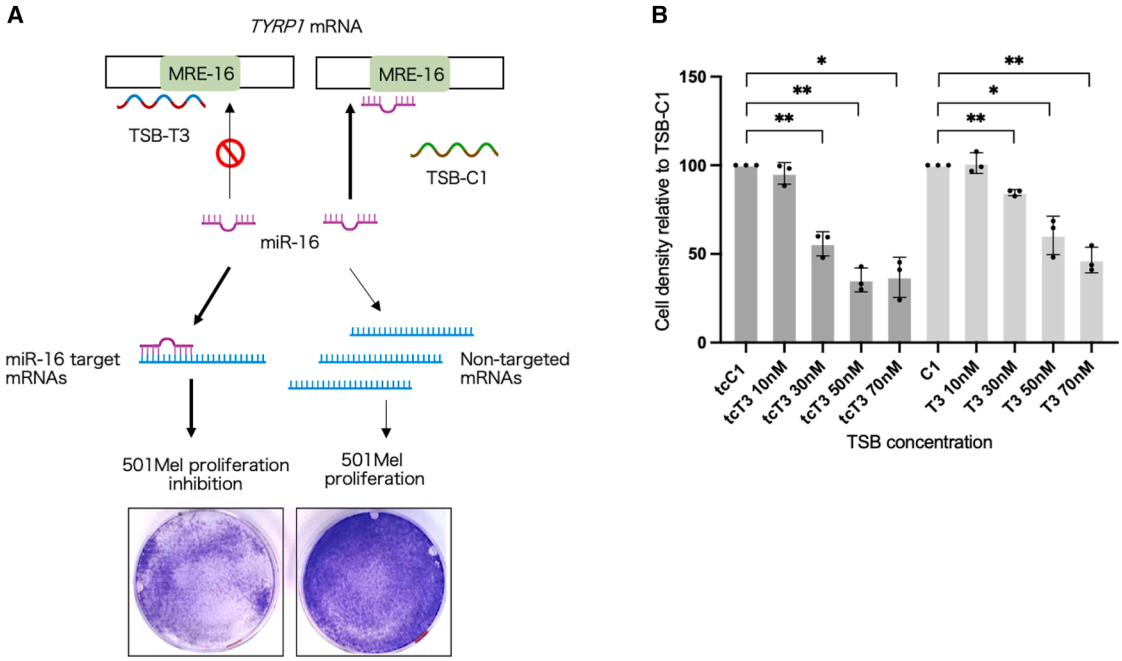

Figure 1. Inhibition of 501Mel cells proliferation with TSB ASOs targeting *TYRP1* mRNA

(A) A competition mechanism occurs with binding of TSB-T3 to a sequence overlapping the miR-16 site in the 3′UTR of *TYRP1* mRNA, thus releasing miR-16 whose tumor suppressor activity is restored. TSB-C1 (Control ASO) has no match with *TYRP1* 3′UTR.[35] The cell density assay upon TSB-C1 or -T3 treatment is measured through a crystal violet colorimetric assay. (A) was generated with BioRender.com. (B) 501Mel cell density assay at day 3 with increasing concentrations of reverse-transfected LNA (T3) or tcDNA (tcT3). Experiments were performed in independent biological triplicates. Data were normalized to the corresponding control conditions (C1 or tcC1) at the same concentrations (10, 30, 50 and 70nM). Data are presented as mean (SD). Unpaired *t* test were performed. The statistical significance is $^{**}p = 0.0040$ (T3 vs. C1 – 30 nM); $^{*}p = 0.0241$ (T3 vs. C1 – 50 nM); $^{**}p = 0.0061$ (T3 vs. C1 – 70 nM); $^{**}p = 0.0078$ (tcT3 vs. tcC1 – 30 nM); $^{**}p = 0.0036$ (tcT3 vs. tcC1 – 50 nM); $^{*}p = 0.0105$ (tcT3 vs. tcC1 – 70 nM).

to ensure that only few cells are transduced with more than one sgRNA and avoid unspecific screening results.[39] With 76,441 sgRNAs and a desired coverage of at least 400 cells per guide, a total of 32 million cells have been transduced and maintained during the screen.

After transduction, cells were positively selected with antibiotic, expanded and subsequently transfected with either the tcT3 or -C1 ASOs. A final ASO concentration of 50 nM was selected based on the former dose-response experiment, which showed that the anti-proliferative effect reached a plateau at this dose (Figure 1B). The treatment was performed for 3 days. After this period, the difference in cell density between the treated and control conditions was greater than 50%.

At the end of treatment, the cells were expanded, pooled and a pellet of 100 million cells per condition was used for genomic DNA (gDNA) extraction and PCR amplification of the integrated sgRNAs in the 3 conditions (non-treated parental cell bank, tcT3 treated and tcC1 treated). The global workflow is depicted in Figure 2A.

After amplicons sequencing by next-generation sequencing (NGS), a quality check was performed and only 115 sgRNAs were not detected over 76,441 in our cell library (0.15%), which validated proper conditions before ASOs treatment. The normalized reads count in each control and therapeutic ASO condition were plotted and provided a mean of 400–500 reads per guide as expected (Figure 2B).

The sequenced sgRNAs coming from the pool of surviving cells after ASO treatment provided information regarding the enriched or depleted ones. Thus, by comparing the sgRNAs enrichment or depletion in treated versus control condition and for each gene, we sought to identify proteins potentially involved in the regulation of ASO uptake, trafficking, release and guidance to their RNA target in this melanoma cell line (Figure 2C).

Identification of tcT3 ASO activity regulators in 501Mel cells

To identify proteins that could impact the tcT3 activity in 501Mel cell line, the NGS sequencing raw data accounting for the total number of sgRNA reads per gene and per sample were analyzed as follows. First, we used MAGeCK count to collect sgRNA read count information from the tcC1- and tcT3-treated cells sequencing files. Then, we used MA Plots to score and identify candidates based on the sgRNA read abundance (A value) and the read counts ratio between the treated and the control condition (M value: fold change [FC]). M and A values were computed for each of the four sgRNAs targeting each individual gene (Figure 3A). From the MA plots, top activator and inhibitor candidates were extracted after using a defined M cut-off for each sgRNA per gene. Figure 3B presents MA plot examples

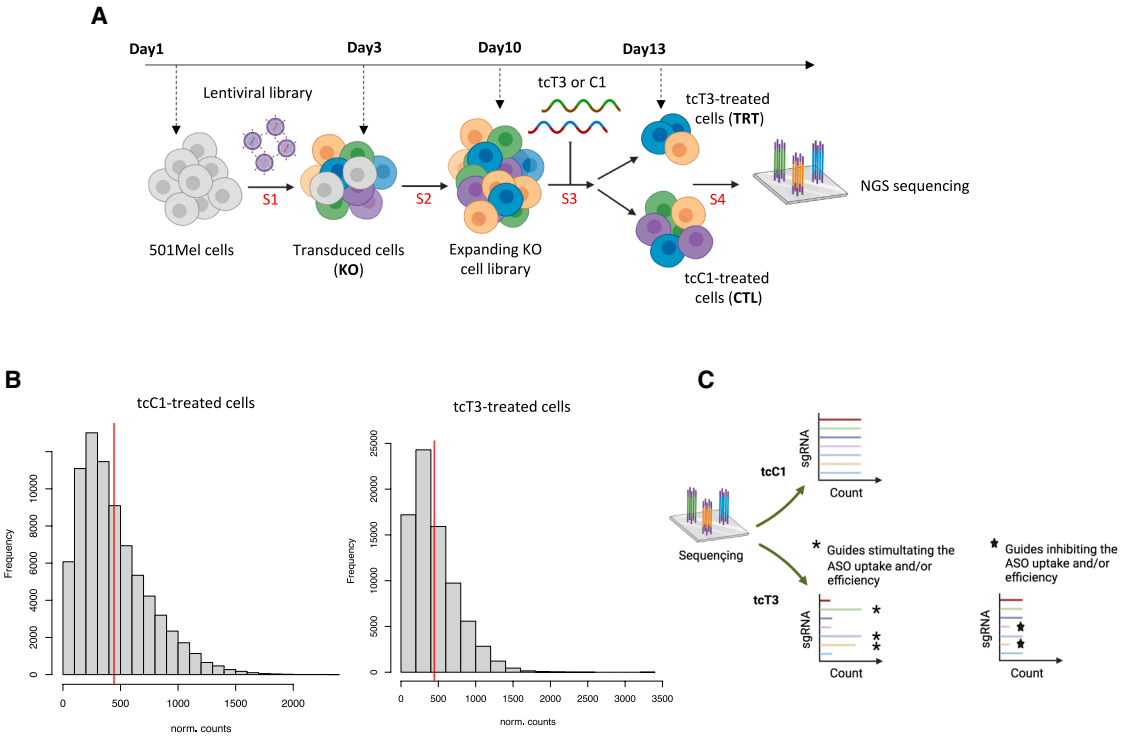

Figure 2. Generation and treatment of the 501Mel cells knockout library

(A) Workflow of the experimental setup. Step 1 (cells transduction – non infected cells in gray on the workflow); Step 2 (transduced cells positive selection with antibiotic); Step 3 (ASO exposure); and Step 4 (gDNA purification and sgRNAs amplification). The figure was generated with BioRender.com (B) Distribution of the number of normalized read counts per sgRNA in the tcT3 and the tcC1-treated library. The mean is represented by a red bar. (C) Method for identifying genes promoting or inhibiting ASO uptake and/or efficiency after NGS sequencing and based on normalized read counts after tcC1 or tcT3 treatment.

from selected activator and inhibitor candidates with applied M cut-off and with four (GGTLC2) or two relevant sgRNAs (WDR91). Because of a short time of treatment (72 h), a minimum FC of 1.5 was fixed between the tcT3 and tcC1 read counts to highlight the best hits (activator candidates: FC tcT3 read counts vs. tcC1 read counts $\geq$1.5; inhibitor candidates: FC tcC1 read counts vs. tcT3 read counts $\geq$1.5) (candidates examples shown in Figure 3C). We opted for a short time of treatment to avoid guide selection bias.

Several sgRNAs targeting the same gene might not have a consistent behavior. However, the Brunello library has been designed with optimized sgRNAs and is known to outperform other knockout libraries.[40] Indeed, the robustness of this library has already been demonstrated with the ability to identify reliable candidates with only two effective sgRNAs per gene.[40] We thus extracted activator and inhibitor candidates considering two, three, or four out of four guides meeting the defined M (FC) and A selection criteria.

As shown in Figures 4A and 4B (and in Table 1), this cutoff allowed to highlight a set of 95 activator candidates and 55 inhibitors. Regarding the activators, 5 genes had their 4 respective sgRNAs fulfilling the corresponding criteria; 28 genes had 3 effective sgRNAs and 62 genes had 2 effective sgRNAs over 4. From the inhibitors, 3, 7, and 45 genes had 4, 3, and 2 effective sgRNAs, respectively. Each of the candidates have been represented by an average FC value; a detailed table of each sgRNA and their respective M, A, and FC values is available in Table 1.

Gene set enrichment analysis using pathway, network and gene set enrichment analysis allowed to classify the activator and inhibitor candidates based on the cellular component gene ontology (Figures S1 and S2).[41] Interestingly, the activator candidates with the highest fold enrichment are mainly clustered within proteins belonging to the peroxisome and mitochondria compartments. Inhibitor candidates are mainly clustered within proteins belonging to the Golgi apparatus and microtubules regulation.

For subsequent validation experiments, we decided to focus on protein activators of ASOs because we were more interested in the mechanistic uptake and trafficking of ASOs in cells. From the list of activators having three effective sgRNAs we highlighted COG8 and RAB5C, two known and well-characterized positive regulators of PS-ASOs productive trafficking and activity in different cell lines.[29,33] This finding further supports the validation and robustness of our screening experiment. As a first set of genes, we selected Elmo domain containing 1 (ELMOD1), fumarate hydratase (FH),

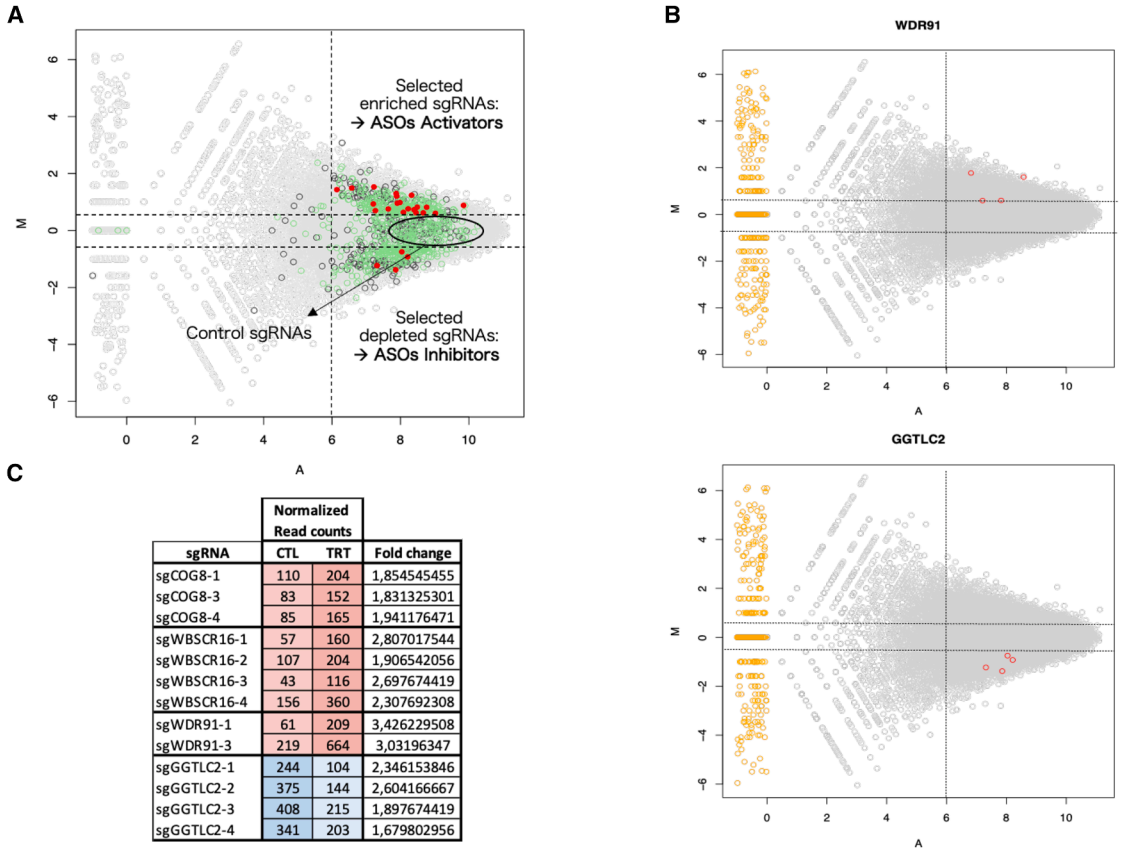

sgRNA	Normalized Read counts CTL	TRT	Fold change
sgCOG8-1	110	204	1,854545455
sgCOG8-3	83	152	1,831325301
sgCOG8-4	85	165	1,941176471
sgWBSCR16-1	57	160	2,807017544
sgWBSCR16-2	107	204	1,906542056
sgWBSCR16-3	43	116	2,697674419
sgWBSCR16-4	156	360	2,307692308
sgWDR91-1	61	209	3,426229508
sgWDR91-3	219	664	3,03196347
sgGGTLC2-1	244	104	2,346153846
sgGGTLC2-2	375	144	2,604166667
sgGGTLC2-3	408	215	1,897674419
sgGGTLC2-4	341	203	1,679802956

Figure 3. NGS sequencing data sorting and analysis

(A) After sgRNA extraction, MA plots are used to visualize the differences between measurements (read counts) between two conditions: treatment (tcT3) versus control (tcC1). For each sgRNA, the read counts are transformed onto M (log ratio) and A (mean average) scales. M is equal to log2(sgRNA_count_in_TRT+1) − log2 (sgRNA_count_in_CTL+1) and A is the mean between count_TRT and count_CTL in log2 scale. Candidates' selection was performed according to the following criteria: $A \geq 6$ and $M \geq 0.6$ (enriched sgRNAs, ASOs activators); $A \geq 6$ and $M \leq -0.6$ (depleted sgRNAs, ASOs inhibitors). Control sgRNAs (non-targeting guides) are located between $M \geq 0.6$ and $M \leq -0.6$. On the obtained MA plot, red, green and black dots represent the genes with the four, three, and two sgRNAs over four fulfilling the defined criteria, respectively (B) MA plot examples from selected activator and inhibitor candidates with applied M and A filters and with four (GGTLC2) or two relevant sgRNAs (WDR91). The yellow dots represent the genes with a very low expression in either the treatment or the control condition and as a consequence, an elevated but non-significant FC (C) Representation of the post-sequencing normalized read counts in the control (CTL – tcC1) and treated (TRT – tcT3) conditions for the sgRNAs of four sorted modulator candidates (COG8, WBSCR16, WDR91, in red – activators; GGTLC2 in blue – inhibitor). The FC is calculated as: tcT3 read counts/tcC1 read counts (for activators); tcC1 read counts/tcT3 read counts (for inhibitors).

transcriptional adapter 2-beta (TADA2B), and Williams-Beuren syndrome chromosome region 16 (WBSCR16), which are from to the top ranked candidates with four sgRNAs fulfilling the chosen criteria. We also selected WDR91 as it is an important factor that participates in the negative regulation of phosphatidylinositol-3-phosphate allowing the early-to-late endosome conversion.[42,43] This first pool of five genes was considered as a nonbiased sampling of potential activator candidates to be further investigated.[44]

WDR91 promotes tcT3-and LNA T3-ASOs activity in 501Mel cells

An RNA interference experiment was designed to further validate the five selected candidates as ASO activity enhancers (Figure 5A). After protein knockdown, the tcT3 activity should be reduced resulting in increased cell proliferation compared to a control condition. It was already well established in previous *in vitro* studies that the protein ANXA2 was an important facilitator of PS-ASOs endosomal trafficking in various cell lines.[34] We thus first evaluated the effect of ANXA2 downregulation in 501Mel cells proliferation with or without tcT3 in comparison with a control siRNA (siCTL). A western blot analysis confirmed the downregulation of ANXA2 protein after cells treatment with an ANXA2 siRNA (Figure S3A). As shown in Figure 5B, *ANXA2* mRNA knockdown significantly impaired the activity of tcT3 by comparison with a control siRNA.

As for ANXA2, each individual candidate (WBSCR16, TADA2B, FH, ELMOD1, and WDR91) was downregulated with a corresponding siRNA (or a control siRNA) for 48 h. The knockdown efficiencies were confirmed by qPCR analysis (Figure S3B) (apart from

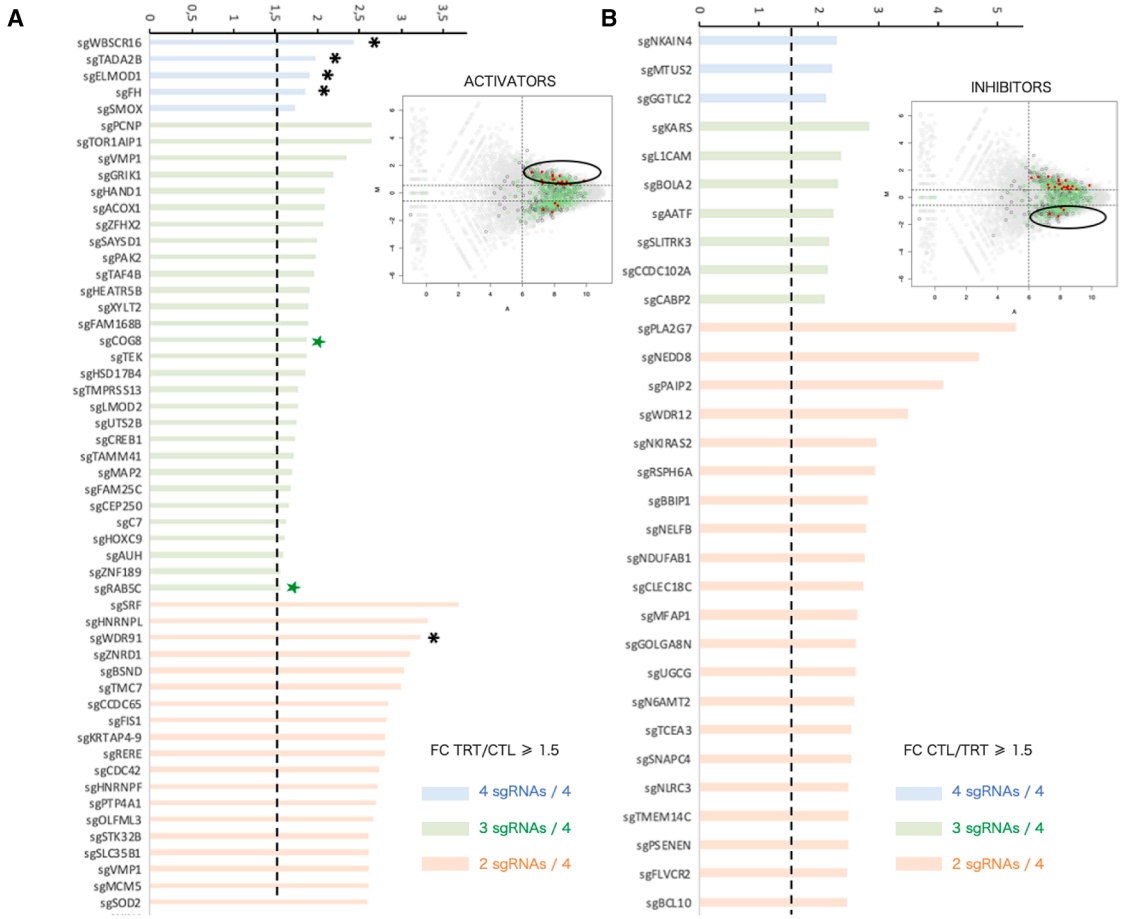

Figure 4. ASO activators and inhibitors ranking and selection

(A) Distribution of the average FC (tcT3 read counts vs. tcC1 read counts) from the FCs of the 2, 3, or 4 corresponding sgRNAs per gene, for 53 of the 95 selected ASO activator candidates (fulfilling the criteria A $\geq$ 6 and M $\geq$ 0.6 on the MA plot). Green stars represent candidates that have already characterized in the literature. Black stars correspond to the five candidates that have been chosen for further functional validation (B) Distribution of the average FC (tcC1 read counts vs. tcT3 read counts) from the FCs of the 2, 3, or 4 corresponding sgRNAs per gene, for 31 of the 55 selected ASO inhibitor candidates (fulfilling the criteria A $\geq$ 6 and M ≤ -0.6 on the MA plot). The FC threshold was fixed to 1.5. The full list of activator and inhibitor candidates is provided in Table 1.

ELMOD1, all knockdowns were shown to be significant enough to allow a relevant biological effect). 501Mel cells were then reverse transfected with either the siRNA alone or a combination of siRNA and tcT3. Four days after the second transfection, the cell density was measured by a crystal violet colorimetric assay (Figure 5B). After normalizing the cell density to each of the corresponding single siRNA treatment, WDR91 and TADA2B knockdowns showed a significant inhibition of tcT3 anti-proliferative activity (Figure 5C; Table S1). Under these conditions, WDR91 knockdown cells showed the most significant and reproducible effect. Therefore, we decided to focus on WDR91 in our further investigations.

We next wondered whether this mechanism was chemistry dependent and carried out the same experiment as above but with the LNA version of the TSB-T3 (instead of tcDNA). Again, under these conditions, ANXA2 and WDR91 knockdowns showed a significant inhibition of the LNA-T3 anti-proliferative activity (Figure 5D; Table S2), indicating that this mechanism was not specific to tcDNA. As for ANXA2, a western blot analysis confirmed the downregulation of WDR91 protein after cells treatment with a WDR91 siRNA (Figure S4A).

Since melanoma cells proliferation can also be promoted by the level of *TYRP1* mRNA expression,[35] we validated by qPCR analysis that *TYRP1* mRNA expression level is not significantly affected by the transfection of control, ANXA2, or WDR91 siRNAs (Figure S4B).

To demonstrate that the knockdown of WDR91 does not affect the total uptake of ASOs in our cells, we conducted a fluorescence experiment by transfecting 501Mel cells with either a control or WDR91 siRNA, followed by the transfection of a FAM-labelled LNA TSB-T3 ASO. Fluorescence imaging analysis revealed a similar signal in

Table 1. List of the ASO activator and inhibitor candidates sorted after applying M, A, and FC filters

Guide	M	A	d	KO	CTL	TRT	FC
sgRNA activator candidates - four guides (A $\geq$ 6 and M $\geq$ 0.6)							
sgELMOD1-1	0.6958466	7.2667865	75	322	121	196	1.6198347
sgELMOD1-2	0.6369571	8.0866629	121	361	218	339	1.5550459
sgELMOD1-3	0.6235261	8.4564213	153	393	283	436	1.540636
sgELMOD1-4	1.5292531	7.2240582	166	178	88	254	2.8863636
sgFH-1	0.6053303	9.0237643	220	718	422	642	1.521327
sgFH-2	0.7281282	8.3974871	172	327	262	434	1.6564885
sgFH-3	1.2947433	7.8761903	218	369	150	368	2.4533333
sgFH-4	0.8187178	8.4915079	207	249	271	478	1.7638376
sgSMOX-1	0.7555813	7.6445772	106	171	154	260	1.6883117
sgSMOX-2	0.6197279	8.667416	176	474	328	504	1.5365854
sgSMOX-3	0.7618403	8.2264102	160	190	230	390	1.6956522
sgSMOX-4	0.9798221	7.9817642	175	318	180	355	1.9722222
sgTADA2B-1	0.8148755	8.7649898	249	281	328	577	1.7591463
sgTADA2B-2	0.8802608	9.8452718	570	821	678	1248	1.840708
sgTADA2B-3	1.2351554	8.3249368	283	295	209	492	2.354067
sgTADA2B-4	0.9574395	7.9049845	162	213	172	334	1.9418605
sgWBSCR16-1	1.4890381	6.5774091	103	171	57	160	2.8070175
sgWBSCR16-2	0.9309584	7.2069462	97	228	107	204	1.9065421
sgWBSCR16-3	1.4317162	6.1421229	73	408	43	116	2.6976744
sgWBSCR16-4	1.2064509	7.8886277	204	451	156	360	2.3076923
sgRNA activator candidates – three guides (A $\geq$ 6 and M $\geq$ 0.6)							
sgACOX1-1	1.0865877	7.1432067	109	91	97	206	2.1237113
sgACOX1-2	0.8549069	8.7673034	262	655	324	586	1.808642
sgACOX1-4	1.1933439	8.6078992	332	416	258	590	2.2868217
sgAUH-2	0.7324145	8.3548919	168	472	254	422	1.6614173
sgAUH-3	0.6228424	9.0461308	230	528	426	656	1.5399061
sgAUH-4	0.6529393	9.1593597	261	619	456	717	1.5723684
sgZNF189-2	0.6429894	8.7008731	187	398	333	520	1.5615616
sgZNF189-3	0.6571123	7.350924	75	195	130	205	1.5769231
sgZNF189-4	0.6205347	9.1368159	244	618	454	698	1.5374449
sgC7-1	0.5912488	8.1348282	116	513	229	345	1.5065502
sgC7-2	0.6367837	8.6358045	177	274	319	496	1.5548589
sgC7-4	0.8353035	8.3305411	189	333	241	430	1.7842324
sgCEP250-1	0.6247301	9.2460557	265	430	489	754	1.5419223
sgCEP250-2	0.7260548	9.552852	382	664	584	966	1.6541096
sgCEP250-4	0.8147345	8.0146975	148	367	195	343	1.7589744
sgCOG8-1	0.8910656	7.2268925	94	367	110	204	1.8545455
sgCOG8-3	0.8728881	6.8114835	69	249	83	152	1.8313253
sgCOG8-4	0.9569313	6.8878566	80	174	85	165	1.9411765
sgCREB1-1	0.7116545	7.4643517	88	248	138	226	1.6376812
sgCREB1-3	0.9640804	7.4127776	116	309	122	238	1.9508197
sgCREB1-4	0.6993405	7.0078817	63	159	101	164	1.6237624
sgZFHX2-2	0.7837915	7.9918086	140	337	194	334	1.7216495

(*Continued on next page*)

Table 1. ***Continued***

Guide	M	A	d	KO	CTL	TRT	FC
sgZFHX2-3	1.3598959	6.5868386	94	130	60	154	2.5666667
sgZFHX2-4	0.9162611	7.513413	118	236	133	251	1.887218
sgFAM168B-1	0.9298122	7.9487219	162	278	179	341	1.9050279
sgFAM168B-2	0.8813555	7.8585303	144	222	171	315	1.8421053
sgFAM168B-3	0.9203406	8.3790335	216	356	242	458	1.892562
sgFAM25C-1	0.6313554	6.988103	56	254	102	158	1.5490196
sgFAM25C-3	0.9268336	6.9712114	82	317	91	173	1.9010989
sgFAM25C-4	0.6568964	7.6771764	94	162	163	257	1.5766871
sgGRIK1-1	1.1431538	7.690518	168	247	139	307	2.2086331
sgGRIK1-2	0.7316124	7.7056562	107	276	162	269	1.6604938
sgGRIK1-3	1.4253058	6.8419359	118	218	70	188	2.6857143
sgHAND1-1	0.7300379	7.7487232	110	181	167	277	1.6586826
sgHAND1-2	0.9682911	7.0077075	88	112	92	180	1.9565217
sgHAND1-4	1.3823007	7.5615151	188	330	117	305	2.6068376
sgHEATR5B-1	0.9083113	8.1194916	178	317	203	381	1.8768473
sgHEATR5B-2	0.7393781	8.2705559	160	367	239	399	1.6694561
sgHEATR5B-3	1.1006324	8.5892352	301	616	263	564	2.1444867
sgHOXC9-1	0.6398244	7.3311395	72	216	129	201	1.5581395
sgHOXC9-2	0.7583174	8.9827851	269	585	389	658	1.6915167
sgHOXC9-4	0.650254	7.495052	82	318	144	226	1.5694444
sgHSD17B4-1	0.6453351	8.7779948	198	452	351	549	1.5641026
sgHSD17B4-2	0.7154095	9.2403478	303	795	472	775	1.6419492
sgHSD17B4-3	1.2322909	6.9911849	112	80	83	195	2.3493976
sgXYLT2-1	1.325958	8.8228503	431	421	286	717	2.506993
sgXYLT2-2	0.6378574	9.2318181	268	547	482	750	1.5560166
sgXYLT2-3	0.6796212	8.7868938	210	264	349	559	1.6017192
sgLMOD2-1	0.6520767	8.3033183	144	542	252	396	1.5714286
sgLMOD2-3	0.6694844	8.731347	199	572	337	536	1.5905045
sgLMOD2-4	1.0959244	8.4548528	273	480	240	513	2.1375
sgMAP2-2	0.617328	7.8860928	102	477	191	293	1.5340314
sgMAP2-3	0.5981194	9.1847561	243	482	473	716	1.5137421
sgMAP2-4	1.0140752	8.501391	260	472	255	515	2.0196078
sgPAK2-1	0.7918918	8.7839632	245	459	335	580	1.7313433
sgPAK2-3	0.980778	8.8997799	331	435	340	671	1.9735294
sgPAK2-4	1.1615891	7.6576102	167	334	135	302	2.237037
sgPCNP-2	1.549687	6.883368	133	232	69	202	2.9275362
sgPCNP-3	1.8875253	6.2656907	108	42	40	148	3.7
sgPCNP-4	0.6305033	8.7373164	188	441	343	531	1.548105
sgSAYSD1-1	0.8573116	8.2295557	181	279	223	404	1.8116592
sgSAYSD1-2	1.2669389	7.5759839	173	204	123	296	2.4065041
sgSAYSD1-3	0.8245233	7.8960774	138	381	179	317	1.7709497
sgTAF4B-2	1.0236513	7.4306889	125	180	121	246	2.0330579
sgTAF4B-3	0.9853532	8.1220332	194	331	198	392	1.979798
sgTAF4B-4	0.8975844	8.070844	170	408	197	367	1.8629442

(*Continued on next page*)

Table 1. *Continued*

Guide	M	A	d	KO	CTL	TRT	FC
sgTAMM41-1	0.6133909	7.3727846	71	310	134	205	1.5298507
sgTAMM41-3	0.8081693	8.3870782	190	313	253	443	1.7509881
sgTAMM41-4	0.8866182	7.8695739	146	627	172	318	1.8488372
sgTEK-2	1.0785691	7.6053737	149	195	134	283	2.1119403
sgTEK-3	0.6268466	9.0616161	234	573	430	664	1.544186
sgTEK-4	0.9549761	7.9613038	168	301	179	347	1.9385475
sgTMPRSS13-1	1.1076683	8.9716867	395	531	342	737	2.1549708
sgTMPRSS13-2	0.6516536	8.6019512	177	520	310	487	1.5709677
sgTMPRSS13-3	0.6668322	9.1503997	265	827	451	716	1.5875831
sgTOR1AIP1-1	0.8596273	8.6682184	246	488	302	548	1.8145695
sgTOR1AIP1-3	0.8280875	8.2405923	176	215	227	403	1.7753304
sgTOR1AIP1-4	2.1609919	6.2504209	125	99	36	161	4.4722222
sgUTS2B-2	0.9805825	8.0371857	182	376	187	369	1.973262
sgUTS2B-3	0.6425732	8.8131397	202	283	360	562	1.5611111
sgUTS2B-4	0.7680761	8.9036743	258	552	367	625	1.7029973
sgVMP1-1	1.4499357	7.3248807	168	439	97	265	2.7319588
sgVMP1-2	0.8605969	5.678226	31	256	38	69	1.8157895
sgVMP1-4	1.3168571	6.4913186	85	286	57	142	2.4912281
sgRNA activator candidates - two guides ($A \geq 6$ and $M \geq 0.6$)							
sgACOX1-1	1.0865877	7.1432067	109	91	97	206	2.1237113
sgACOX1-4	1.1933439	8.6078992	332	416	258	590	2.2868217
sgACVR1B-3	1.007342	8.1183808	198	357	196	394	2.0102041
sgACVR1B-4	1.2302976	6.3155885	70	105	52	122	2.3461538
sgAXIN1-1	1.6241686	7.7309475	252	162	121	373	3.0826446
sgAXIN1-4	1.0143553	7.7359963	153	225	150	303	2.02
sgBRI3BP-1	1.0336593	8.3810158	244	273	233	477	2.0472103
sgBRI3BP-2	1	6.6085245	69	72	69	138	2
sgBSND-2	1.2103599	8.0314447	226	387	172	398	2.3139535
sgBSND-4	1.9125372	6.0437314	94	132	34	128	3.7647059
sgCBWD6-2	1.1885777	7.3887047	142	295	111	253	2.2792793
sgCBWD6-3	1.0703893	7.1790509	110	580	100	210	2.1
sgCCDC65-1	1.277781	6.8287151	104	258	73	177	2.4246575
sgCCDC65-4	1.7045441	6.6071596	122	212	54	176	3.2592593
sgCCL4L2-2	1.0404791	7.462754	130	359	123	253	2.0569106
sgCCL4L2-4	1.4150375	7.7843343	225	269	135	360	2.6666667
sgCDC42-2	1.7288377	7.3401523	206	417	89	295	3.3146067
sgCDC42-4	1.1139562	6.7468027	85	505	73	158	2.1643836
sgCHERP-3	1.0324215	7.2975705	115	535	110	225	2.0454545
sgCHERP-4	1.1667784	7.2558146	127	368	102	229	2.245098
sgCHURC1-FNTB-1	1.1016954	7.0265811	102	718	89	191	2.1460674
sgCHURC1-FNTB-3	1.4739312	6.7142455	112	611	63	175	2.7777778
sgCIAO1-3	1.0588937	6.9217643	91	519	84	175	2.0833333
sgCIAO1-4	1.5215371	6.7149649	116	452	62	178	2.8709677
sgCNR1-2	1.017848	8.4218133	247	375	241	488	2.0248963

(*Continued on next page*)

Table 1. ***Continued***

Guide	M	A	d	KO	CTL	TRT	FC
sgCNR1-3	1.122374	8.8138524	359	320	305	664	2.1770492
sgCSTB-3	1.16711	7.416445	142	354	114	256	2.245614
sgCSTB-4	1.5077946	6.7538973	118	252	64	182	2.84375
sgDEFB135-1	1.4139572	8.0906829	278	358	167	445	2.6646707
sgDEFB135-4	1.0584597	7.5845123	144	330	133	277	2.0827068
sgEED-1	1.1737366	7.9791857	211	466	168	379	2.2559524
sgEED-2	1.4666199	8.2411046	321	217	182	503	2.7637363
sgERVFRD-1-3	1.1425391	7.5936374	157	138	130	287	2.2076923
sgERVFRD-1-4	1.0366585	7.6057921	143	227	136	279	2.0514706
sgEXT2-1	1.0484101	9.9208098	720	908	674	1394	2.0682493
sgEXT2-2	1.1969155	8.5814513	327	352	253	580	2.2924901
sgEXTL3-2	1.3345683	9.6330684	761	352	500	1261	2.522
sgEXTL3-3	1.2886643	9.9274205	899	515	623	1522	2.4430177
sgFANCC-2	1.2113089	7.9979719	221	191	168	389	2.3154762
sgFANCC-3	1.3475043	7.6162667	190	205	123	313	2.5447154
sgFIS1-1	1.052321	7.9855921	189	424	176	365	2.0738636
sgFIS1-3	1.8405218	6.3465256	111	731	43	154	3.5813953
sgGABBR1-1	1.1755716	7.9971767	214	213	170	384	2.2588235
sgGABBR1-4	1.0378682	8.0735229	198	305	188	386	2.0531915
sgGRIK1-1	1.1431538	7.690518	168	247	139	307	2.2086331
sgGRIK1-3	1.4253058	6.8419359	118	218	70	188	2.6857143
sgHNRNPF-1	1.3219281	6.3048202	75	205	50	125	2.5
sgHNRNPF-4	1.5484366	6.0961464	77	139	40	117	2.925
sgHNRNPL-3	2.0202724	6.7380567	162	362	53	215	4.0566038
sgHNRNPL-4	1.3572951	8.7766797	428	848	274	702	2.5620438
sgICOSLG-3	1.0783162	8.4580214	269	333	242	511	2.1115702
sgICOSLG-4	1.1982696	7.4064897	145	272	112	257	2.2946429
sgKRTAP4-9-2	1.7432246	6.3951742	108	229	46	154	3.3478261
sgKRTAP4-9-4	1.177193	7.0480281	111	179	88	199	2.2613636
sgLCP1-1	1.0192791	8.3105394	229	303	223	452	2.0269058
sgLCP1-2	1.2638123	8.9033692	433	468	309	742	2.4012945
sgMCM5-1	1.4277486	7.5340532	191	527	113	304	2.6902655
sgMCM5-2	1.3393853	7.5151827	176	522	115	291	2.5304348
sgMETAP1-1	1.0553768	7.3731784	124	349	115	239	2.0782609
sgMETAP1-4	1.1938797	6.7867644	94	364	73	167	2.2876712
sgNKX2-4-2	1.0571954	7.6160605	147	173	136	283	2.0808824
sgNKX2-4-3	1.020716	8.4292212	249	260	242	491	2.0289256
sgNRD1-1	1.2446739	8.6279615	352	480	257	609	2.3696498
sgNRD1-4	1.2132032	7.6834172	178	325	135	313	2.3185185
sgOLFML3-1	1.284096	7.0514389	122	329	85	207	2.4352941
sgOLFML3-4	1.5398105	7.664723	227	262	119	346	2.907563
sgOR2L5-3	1.4742034	8.4650221	377	422	212	589	2.7783019
sgOR2L5-4	1.1604647	6.6676952	84	56	68	152	2.2352941
sgOR4C12-3	1.2410081	6.8872906	105	214	77	182	2.3636364

(*Continued on next page*)

Table 1. *Continued*

Guide	M	A	d	KO	CTL	TRT	FC
sgOR4C12-4	1.0074175	8.6885841	294	388	291	585	2.0103093
sgPKLR-1	1.254138	7.5578063	169	220	122	291	2.3852459
sgPKLR-4	1.0901978	7.0842577	105	322	93	198	2.1290323
sgPOC1A-1	1.3219281	6.8704174	111	240	74	185	2.5
sgPOC1A-4	1.0402639	7.2480524	112	495	106	218	2.0566038
sgPOF1B-2	1.226915	7.1212521	122	146	91	213	2.3406593
sgPOF1B-4	1.4065059	7.4311734	175	269	106	281	2.6509434
sgPRSS53-2	1.1643868	7.0251369	108	183	87	195	2.2413793
sgPRSS53-3	1.4489848	6.7017723	109	131	63	172	2.7301587
sgPSMA1-2	1.0631938	6.5976861	73	345	67	140	2.0895522
sgPSMA1-4	1.2644156	7.0751513	122	273	87	209	2.4022989
sgPTP4A1-1	1.6114347	6.5606049	111	181	54	165	3.0555556
sgPTP4A1-2	1.2337972	6.3717861	73	108	54	127	2.3518519
sgRERE-1	1.6412699	6.8867242	142	366	67	209	3.119403
sgRERE-4	1.3136605	7.3710758	156	195	105	261	2.4857143
sgRPS14-2	3.5443205	3.3571228	32	28	3	35	11.666667
sgRPS14-3	1.5589673	6.5868386	109	243	56	165	2.9464286
sgSLC35B1-1	1.3362834	8.5750323	366	911	240	606	2.525
sgSLC35B1-4	1.4329594	6.0384078	68	217	40	108	2.7
sgSLC39A9-3	1.0524674	7.6030493	145	438	135	280	2.0740741
sgSLC39A9-4	1.0193468	10.527874	1065	901	1037	2102	2.027001
sgSLC5A7-1	1.0329146	6.5388251	68	112	65	133	2.0461538
sgSLC5A7-3	1.1043367	8.4590589	276	382	240	516	2.15
sgSOD2-1	1.4296843	7.329552	166	160	98	264	2.6938776
sgSOD2-3	1.3219281	6.3048202	75	191	50	125	2.5
sgSPDYE2-1	1.017403	8.1952021	211	341	206	417	2.0242718
sgSPDYE2-3	1.0740006	6.7849278	84	477	76	160	2.1052632
sgSRF-2	2.194378	5.7976287	93	594	26	119	4.5769231
sgSRF-4	1.4788341	6.2940059	84	293	47	131	2.787234
sgSTK32B-1	1.3245252	7.4566785	167	270	111	278	2.5045045
sgSTK32B-2	1.4484605	7.3091928	166	294	96	262	2.7291667
sgTELO2-1	1.0919225	6.7938888	86	424	76	162	2.1315789
sgTELO2-2	1.1443899	6.405085	69	576	57	126	2.2105263
sgTLCD1-2	1.2459792	6.9083918	107	169	78	185	2.3717949
sgTLCD1-3	1.0673553	7.6211405	149	378	136	285	2.0955882
sgTMC7-2	1.9237644	6.049345	95	56	34	129	3.7941176
sgTMC7-4	1.1375035	7.1386074	114	397	95	209	2.2
sgTMEM131-2	1.3487282	6.6743641	99	243	64	163	2.546875
sgTMEM131-3	1.1672947	6.5143847	76	189	61	137	2.2459016
sgUBALD1-2	1.0038116	8.0641482	190	269	189	379	2.005291
sgUBALD1-4	1.0949484	7.7471465	167	569	147	314	2.1360544
sgUQCRB-3	1.5849625	6.573841	110	240	55	165	3
sgUQCRB-4	1.0448542	8.0922827	202	386	190	392	2.0631579
sgVMP1-1	1.4499357	7.3248807	168	439	97	265	2.7319588

(*Continued on next page*)

Table 1. *Continued*

Guide	M	A	d	KO	CTL	TRT	FC
sgVMP1-4	1.3168571	6.4913186	85	286	57	142	2.4912281
sgVSTM5-3	1.3138908	6.8268704	107	236	72	179	2.4861111
sgVSTM5-4	1.3858912	6.9217643	121	240	75	196	2.6133333
sgWDR91-1	1.7766218	6.8190482	148	69	61	209	3.4262295
sgWDR91-3	1.6002524	8.5749132	445	277	219	664	3.0319635
sgZNF492-2	1.2505435	7.4832527	160	217	116	276	2.3793103
sgZNF492-3	1.1901029	6.7447986	91	275	71	162	2.2816901
sgZNRD1-1	1.8559897	6.571851	131	635	50	181	3.62
sgZNRD1-4	1.3706434	7.3146783	157	412	99	256	2.5858586
sgRNA inhibitor candidates – four guides (A $\geq$ 6 and M $\leq$ −0.6)							
sgGGTLC2-1	−1.230298	7.3155885	−140	301	244	104	2.3461538
sgGGTLC2-2	−1.380822	7.8603359	−231	287	375	144	2.6041667
sgGGTLC2-3	−0.924232	8.2103091	−193	230	408	215	1.8976744
sgGGTLC2-4	−0.748292	8.0394819	−138	374	341	203	1.679803
sgMTUS2-1	−1.366782	4.9313187	−30	100	49	19	2.5789474
sgMTUS2-2	−1.090198	6.4992952	−70	157	132	62	2.1290323
sgMTUS2-3	−1.411314	7.30557	−161	348	258	97	2.6597938
sgMTUS2-4	−0.59172	6.4456071	−36	156	107	71	1.5070423
sgNKAIN4-1	−0.787885	8.9369743	−271	616	644	373	1.7265416
sgNKAIN4-2	−1.308922	8.9398634	−461	460	773	312	2.4775641
sgNKAIN4-3	−1.04891	7.9673983	−186	220	360	174	2.0689655
sgNKAIN4-4	−1.554589	5.7772944	−62	55	94	32	2.9375
sgRNA inhibitor candidates – three guides (A $\geq$ 6 and M $\leq$ −0.6)							
sgAATF-1	−1.301464	6.8004791	−104	239	175	71	2.4647887
sgAATF-2	−0.619095	7.8093935	−97	195	278	181	1.5359116
sgAATF-3	−1.47592	7.1809034	−155	419	242	87	2.7816092
sgBOLA2-1	−1.657112	7.9884275	−308	121	451	143	3.1538462
sgBOLA2-2	−1.194816	6.9724475	−107	255	190	83	2.2891566
sgBOLA2-3	−0.610498	7.1126037	−59	322	171	112	1.5267857
sgCABP2-1	−1.247928	7.6239638	−176	350	304	128	2.375
sgCABP2-3	−1.152599	7.4951628	−148	386	269	121	2.2231405
sgCABP2-4	−0.753839	7.049345	−70	249	172	102	1.6862745
sgCCDC102A-1	−1.078003	7.9568538	−190	378	361	171	2.1111111
sgCCDC102A-2	−0.740913	6.5602809	−49	61	122	73	1.6712329
sgCCDC102A-4	−1.436099	6.8055124	−116	218	184	68	2.7058824
sgKARS-1	−1.417767	8.3382403	−331	548	529	198	2.6717172
sgKARS-2	−1.609416	6.09011	−80	566	119	39	3.0512821
sgKARS-3	−1.494765	5.7917765	−60	447	93	33	2.8181818
sgSLITRK3-1	−1.426265	7.2980949	−162	172	258	96	2.6875
sgSLITRK3-2	−1.176453	9.2029364	−494	873	886	392	2.2602041
sgSLITRK3-3	−0.63743	9.48864	−320	744	896	576	1.5555556
sgL1CAM-1	−1.093867	7.4417512	−135	161	254	119	2.1344538
sgL1CAM-2	−1.788872	7.5526474	−248	238	349	101	3.4554455
sgL1CAM-3	−0.606336	8.9542198	−210	422	612	402	1.5223881

(*Continued on next page*)

Table 1. *Continued*

Guide	M	A	d	KO	CTL	TRT	FC
sgRNA inhibitor candidates – two guides (A $\geq$ 6 and M $\leq$ −0.6)							
sgACOT8-2	−1.182864	6.8008854	−94	124	168	74	2.2702703
sgACOT8-3	−1.214878	7.9737614	−218	274	383	165	2.3212121
sgARHGEF2-2	−1.186096	7.7015726	−176	275	314	138	2.2753623
sgARHGEF2-3	−1.246966	7.9272638	−217	357	375	158	2.3734177
sgCASP5-3	−1.04182	7.1933354	−108	208	210	102	2.0588235
sgCASP5-4	−1.285909	6.832779	−105	160	178	73	2.4383562
sgCCDC51-2	−1.284453	7.5125914	−168	185	285	117	2.4358974
sgCCDC51-4	−1.059334	7.5630901	−142	97	273	131	2.0839695
sgCLEC18C-1	−1.657112	4.5289959	−28	63	41	13	3.1538462
sgCLEC18C-3	−1.232661	7.2601866	−135	239	235	100	2.35
sgFAM86B1-2	−1.153079	6.6426289	−82	238	149	67	2.2238806
sgFAM86B1-4	−1.395929	7.2678199	−155	312	250	95	2.6315789
sgKRT20-2	−0.763197	8.1497829	−152	368	370	218	1.6972477
sgKRT20-3	−0.604862	6.8873935	−50	403	146	96	1.5208333
sgLILRA6-1	−1.079727	6.9992952	−98	142	186	88	2.1136364
sgLILRA6-4	−1.04858	8.2990771	−234	447	453	219	2.0684932
sgMRPL52-1	−1.398549	7.4806344	−180	379	290	110	2.6363636
sgMRPL52-4	−1.021695	6.5552417	−68	249	134	66	2.030303
sgNEDD8-3	−2.807355	3.7256056	−30	633	35	5	7
sgNEDD8-4	−1.258734	7.4367221	−156	570	268	112	2.3928571
sgNELFB-2	−0.671578	7.7194934	−99	396	266	167	1.5928144
sgNELFB-4	−2.004738	7.2502965	−229	480	305	76	4.0131579
sgRDH11-1	−1.291582	8.4336937	−320	341	541	221	2.4479638
sgRDH11-2	−1.224291	8.3736966	−290	191	507	217	2.3364055
sgSF3A2-2	−1.065724	7.4155051	−129	116	247	118	2.0932203
sgSF3A2-4	−1.050626	7.332668	−120	411	232	112	2.0714286
sgSNAPC4-1	−1.104337	4.8740964	−23	225	43	20	2.15
sgSNAPC4-2	−1.563429	7.2735678	−176	304	266	90	2.9555556
sgSSRP1-1	−1.20581	6.8317235	−98	226	173	75	2.3066667
sgSSRP1-2	−1.179133	8.7941377	−373	425	668	295	2.2644068
sgTUBG1-3	−1.252387	5.7136564	−47	304	81	34	2.3823529
sgTUBG1-4	−1.163348	7.9995265	−212	729	383	171	2.2397661
sgGOLGA8*N*-2	−1.39486	7.4523173	−176	165	284	108	2.6296296
sgGOLGA8*N*-4	−1.389042	6.6718011	−102	199	165	63	2.6190476
sgHMBS-1	−1.00946	6.7526577	−77	222	153	76	2.0131579
sgHMBS-4	−1.39486	7.0372798	−132	218	213	81	2.6296296
sgKLK14-1	−0.85561	7.6274774	−119	276	266	147	1.8095238
sgKLK14-4	−1.092824	7.8501928	−179	347	337	158	2.1329114
sgMFAP1-1	−1.348895	6.402368	−82	246	135	53	2.5471698
sgMFAP1-3	−1.463947	6.5899545	−102	222	160	58	2.7586207
sgNDUFAB1-1	−1.096215	5.4060887	−33	87	62	29	2.137931
sgNDUFAB1-4	−1.777608	6.6961587	−136	257	192	56	3.4285714
sgNKIRAS2-3	−1.836501	6.7256056	−144	170	200	56	3.5714286

(*Continued on next page*)

Table 1. *Continued*

Guide	M	A	d	KO	CTL	TRT	FC
sgNKIRAS2-4	−1.24664	6.505963	−81	175	140	59	2.3728814
sgNPR3-1	−1.353637	7.6540984	−196	301	322	126	2.5555556
sgNPR3-2	−1.123896	8.0855102	−217	378	401	184	2.1793478
sgPAIP2-3	−1.592825	6.7271496	−123	27	184	61	3.0163934
sgPAIP2-4	−2.365181	6.7061526	−191	99	237	46	5.1521739
sgREEP2-2	−1.192645	8.0475337	−225	139	400	175	2.2857143
sgREEP2-4	−1.007777	8.0352701	−187	259	372	185	2.0108108
sgRSPH6A-1	−1.597563	6.0467088	−77	120	115	38	3.0263158
sgRSPH6A-4	−1.524421	7.952035	−274	270	420	146	2.8767123
sgTCEA3-1	−1.5025	6.1435676	−77	184	119	42	2.8333333
sgTCEA3-2	−1.185279	7.6694552	−172	166	307	135	2.2740741
sgTMEM14C-1	−1.073249	8.121587	−212	382	404	192	2.1041667
sgTMEM14C-3	−1.523562	7.2212126	−165	287	253	88	2.875
sgTRAFD1-1	−1.463247	7.4181238	−181	309	284	103	2.7572816
sgTRAFD1-4	−1.119299	6.4176305	−68	108	126	58	2.1724138
sgUGCG-1	−1.065095	6.5549153	−71	179	136	65	2.0923077
sgUGCG-2	−1.649379	7.0145142	−156	77	229	73	3.1369863
sgWDR12-1	−2.039528	6.9970441	−196	248	259	63	4.1111111
sgWDR12-3	−1.534777	6.0527906	−74	93	113	39	2.8974359
sgN6AMT2-1	−1.532495	7.8955306	−265	138	405	140	2.8928571
sgN6AMT2-3	−1.214682	7.67343	−177	152	311	134	2.3208955
sgNLRC3-2	−1.504994	6.8399599	−125	88	193	68	2.8382353
sgNLRC3-3	−1.117039	6.7082668	−83	216	154	71	2.1690141
sgPLA2G7-1	−3.006919	6.2038994	−183	191	209	26	8.0384615
sgPLA2G7-2	−1.389706	7.9986339	−256	318	414	158	2.6202532
sgPSENEN-3	−1.20112	8.5312971	−317	490	561	244	2.2991803
sgPSENEN-4	−1.420181	7.4243359	−176	470	281	105	2.6761905
sgRSF1-1	−1.030261	9.162589	−418	640	819	401	2.042394
sgRSF1-4	−1.193604	7.1513909	−121	178	215	94	2.287234
sgSTK11-1	−1.217029	6.8753012	−102	386	179	77	2.3246753
sgSTK11-4	−1.237039	6.7478026	−95	236	165	70	2.3571429
sgTMPRSS2-2	−1.188762	7.1335396	−119	159	212	93	2.2795699
sgTMPRSS2-3	−1.273018	6.5433998	−85	96	145	60	2.4166667
sgXKR4-2	−1.347019	6.5063996	−88	185	145	57	2.5438596
sgXKR4-3	−1.072569	7.5135642	−139	341	265	126	2.1031746
sgBBIP1-2	−1.407175	6.2271496	−76	130	122	46	2.6521739
sgBBIP1-4	−1.591915	6.9044821	−139	211	208	69	3.0144928
sgATP6V0D2-1	−1.051193	8.5645157	−282	303	545	263	2.0722433
sgATP6V0D2-2	−1.341037	6.8993371	−115	75	190	75	2.5333333
sgBCL10-3	−1.532221	6.7884783	−123	218	188	65	2.8923077
sgBCL10-4	−1.028855	7.1437841	−103	137	202	99	2.040404
sgC1orf158-1	−1.181838	8.9789364	−425	422	760	335	2.2686567
sgC1orf158-4	−1.007777	8.0352701	−187	289	372	185	2.0108108
sgCPSF4L-2	−0.554031	8.058375	−103	314	323	220	1.4681818

(*Continued on next page*)

Table 1. *Continued*

Guide	M	A	d	KO	CTL	TRT	FC
sgCPSF4L-4	−1.241376	7.8590925	−206	318	357	151	2.3642384
sgFLVCR2-3	−1.053111	8.6558387	−301	515	581	280	2.075
sgFLVCR2-4	−1.525827	7.1379531	−156	218	239	83	2.8795181

The corresponding 95 and 55 activator and inhibitor candidates are represented with their respective sgRNAs fulfilling the defined criteria. M (log ratio) = log2 (sgRNA_count_in_TRT+1) − log2(sgRNA_count_in_CTL+1); A (Mean average) = mean (count_TRT, count_CTL) in log2 scale. Fold-changes (FC) between TRT (tcT3-treated cells) and CTL (tcC1-treated cells) conditions were computed from the M values of each sgRNA as FC (activator) = TRT read counts/CTL read counts; FC (inhibitor) = CTL read counts/TRT read counts. KO is the number of read counts in the parental non-treated knockout library. d value represents the absolute difference between the CTL and the TRT read counts.

both conditions, showing that the inhibition of WDR91 does not significantly affect the total uptake of ASO into cells (Figure 5E).

WDR91 enhancer activity is validated in other cell lines and with different ASO modalities

We identified WDR91 in melanoma cells using a fully modified TSB ASO and wondered whether similar effects would hold true in a different system (different mechanism of action and cell line). Indeed, it is known that human cancer cell lines have very heterogeneous ASO uptake efficiencies. To address this question, we first transfected the U2OS osteosarcoma cell line with siRNAs (control or directed against ANXA2 or WDR91) and evaluated the effect on LNA GMs activity (inducing mRNA knockdown) directed against metastasis-associated lung adenocarcinoma transcript 1 (*MALAT1*) and inhibitor of growth family member 2 (*ING2*) RNAs. From these two RNAs, *MALAT1* is a highly studied and conserved nuclear long non-coding RNA and is expressed in many cells. The experimental workflow is depicted in Figure 6A.

In this cell line, RT-qPCR in control-siRNA conditions confirmed the efficient downregulation of *MALAT1* and *ING2* mRNAs by their respective GM (Figure 6B). Surprisingly, downregulation of ANXA2 did not impair the effect of MALAT1 or ING2 GM, as was expected (Figure 6B). Yet, we observed that WDR91 knockdown efficiently abrogated MALAT1 ASO activity (Figure 6C), confirming the putative role of this protein in ASO potency. However, no such effect was observed on ING2 ASO activity (Figure 6C). Of note, both 16-mers MALAT1 and ING2 GMs have the same design and chemistry and only differ by their respective sequence. To investigate this difference of activity between the two GMs, we compared the expression levels of *MALAT1* and *ING2* mRNAs in non-treated cells and found that the *ING2* mRNA levels were significantly higher compared with *MALAT1* mRNA levels (Figure S5). This difference in expression levels in the U2OS cells might explain the discrepancies observed between MALAT1 and ING2 GMs treatments within our experimental setup.

To further confirm the activity of WDR91, we conducted a validation experiment with MALAT1 GM using an additional cancer cell line, the PC9 pulmonary adenocarcinoma cell line. As shown in Figure 6D and as previously observed in U2OS cells, downregulation of ANXA2 did not impact the activity of the MALAT1 GM in PC9 cells. We thus included RAB5C, another characterized positive regulator of ASOs productive trafficking and activity that was highlighted in our CRISPR screen. The downregulation of RAB5C significantly impacted MALAT1 ASO-mediated mRNA knockdown in PC9 cells, validating our experimental setup (Figure 6D). We then evaluated the impact of WDR91 downregulation in PC9 cells and confirmed that it efficiently abrogated MALAT1 ASO activity (Figure 6E). Together, these data highlight for the first time the protein WDR91 as an ASO regulator and in a physiological context. This activity has been confirmed in three distinct cell lines.

WDR91 does not influence ASOs activity in muscle cells

To evaluate the potency of WDR91 to affect PS-ASOs activity in a different context, we assessed WDR91's ability to influence the activity of a splice-switching ASO used to mediate exon skipping in skeletal muscle cells. ASO-mediated exon-skipping is indeed one of the most promising therapeutic approaches for the treatment of Duchenne muscular dystrophy (DMD). The mechanism of action of ASO in this context is to mask important regulatory splicing signals to exclude the targeted exon and restore the reading frame of the DMD pre-mRNA.[45] Immortalized human myoblasts from DMD patients are typically used as a model to study dystrophin restoration mediated by splice switching oligonucleotides (SSOs). Here we used immortalized DMD myoblasts carrying a deletion of DMD exon 52 leading to an out-of-frame mRNA and resulting in the absence of dystrophin. The use of an SSO directed against the exon 51 (SSOEx51) allows to restore the open reading frame of the dystrophin mRNA.

To study the effect of WDR91 on SSOEx51 activity, the immortalized KM571 cells were first transfected with siRNAs to knockdown WDR91 or ANXA2 expression (Figure 7A). Seventy-two hours later, cells were treated with the SSOEx51 (LNA/2′MOE PS mixmer) to study exon 51 skipping efficiency in a context where WDR91 or ANXA2 expression was reduced. RNA was extracted to first check knockdown efficiency, and we confirmed that siRNAs treatment resulted in a strong knockdown (>70%) of *WDR91* and *ANXA2* respective mRNAs (Figure 7B). Exon skipping levels were then compared and normalized to the siCTL. We noted a significant reduction in the exon skipping efficacy when ANXA2 expression was reduced (Figure 7C). However,

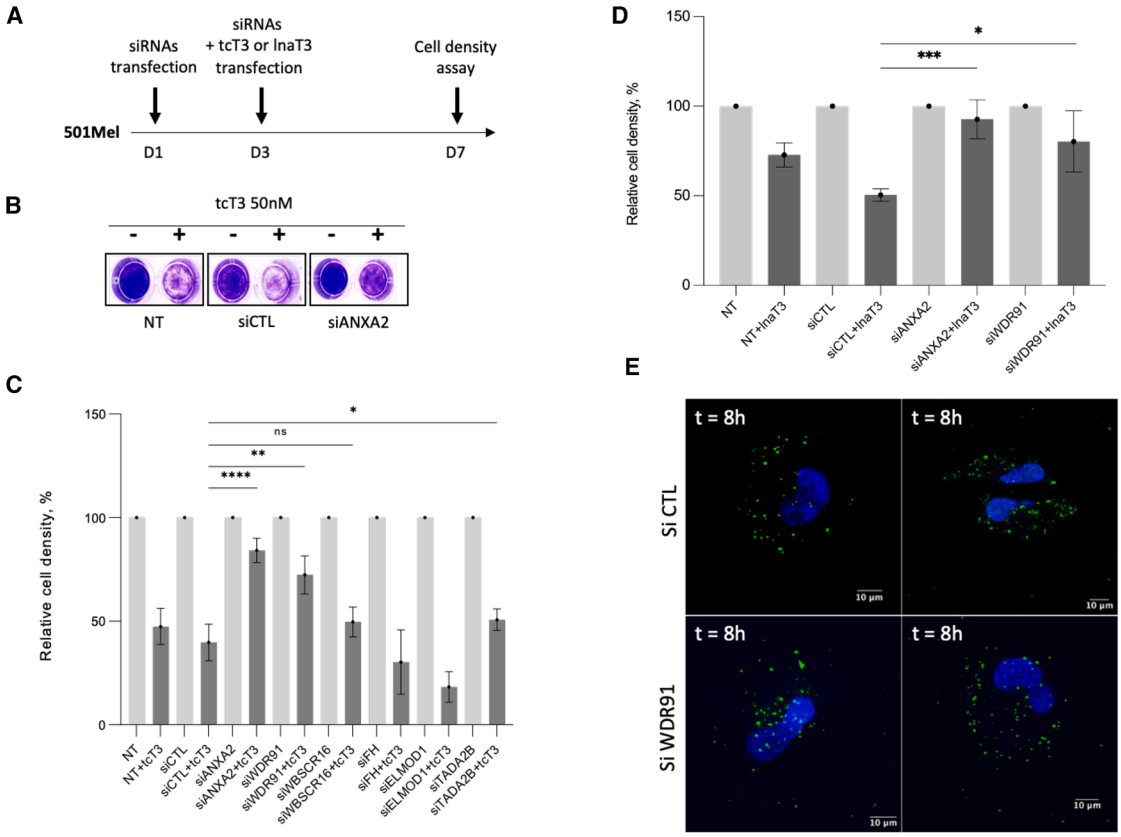

Figure 5. Functional validation of tcT3 and lnaT3 activity enhancer candidates in 501Mel cells and confocal microscopy experiment

(A) Workflow of the experimental design. (B) Setup of the 501Mel cell density assay with ANXA2 positive control. Cell density measurement was performed by crystal violet assay after tcT3 transfection on normal, control or ANXA2 knockdown cells, NT, non-treated. The relative cell density in each condition is normalized to the NT cells. (C) 501Mel cell density assay after tcT3 transfection on normal, control, or candidate's knockdown cells. Data are presented with a cell density normalized to 100% for each treatment with the siRNA alone, to discard any proliferation bias induced by the siRNA's effects. (D) 501Mel cell density assay after LNA T3 transfection on normal, control, WDR91 or ANXA2 knockdown cells. Data are presented with a cell density normalized to 100% for each treatment with the siRNA alone, to discard any proliferation bias induced by the siRNA's effects. (E) Confocal microscopy of 501Mel cells, transfected with either a control or a WDR91 siRNA and then with 50 nM of a FAM-labelled LNA TSB T3 ASO (Blue: Hoechst 33258 - nucleus; Green: FAM-labelled LNA TSB T3 ASO). Scale bar, 10 µm. Experiments were performed in independent biological replicates. Data are presented as mean (SD). Unpaired *t* tests were performed. The statistical significance is (C): $^{*}p = 0.0468$ (TADA2B, $n = 3$); $^{**}p = 0.0011$ (WDR91, $n = 4$); $^{****}p \leq 0.0001$ (ANXA2, $n = 5$); NS = non-significant ($p = 0.0588$); (D): $^{*}p = 0.0154$ (WDR91, $n = 5$); $^{***}p = 0.0004$ (ANXA2, $n = 5$).

this effect was not observed with WDR91. Similar results were obtained with the two other SSO chemistries investigated (2′MOE-PS and tcDNA-PS) (Figure S6A), indicating that WDR91 is not a modulator of ASO activity in this system. To exclude a potential sequence specific effect, we also confirmed these results with an SSO targeting *DMD* exon 53, whose effect was impacted by the knockdown of ANXA2 but not WDR91 (Figure S6B).

To determine whether this effect was specific to SSOs or to KM571 cells, we used a different type of ASO to clarify the role of WDR91 in these cells. As described above, we first transfected the KM571 cells with siRNAs targeting *WDR91* or *ANXA2* mRNAs and then with a GM against *ING2* mRNA (GM ING2) (Figure 7D). Here again, siRNA-induced knockdown of *WDR91* and *ANXA2* was very efficient (Figure 7E). When quantifying the levels of *ING2* mRNA, we confirmed the effect of the positive control ANXA2 but observed no significant differences between the siRNA-control and siRNA-WDR91 treatments (Figure 7F) indicating that WDR91 knockdown did not affect GM ING2 activity. These results suggest that WDR91 likely does not contribute to ASO activity in KM571 cells, regardless of the type of PS-ASOs used (SSO or GM).

DISCUSSION

Despite many clinical successes, the precise mechanisms of ASO uptake and trafficking remain to be fully understood. In this study, we used a genome-wide CRISPR inhibition screen to identify without *a priori* proteins involved in PS-ASO trafficking, release, and productive activity in a 501Mel cell line. Our CRISPR knockout screening strategy has enabled us to discover functionally involved proteins, using a third-generation ASO and preserving the integrity of

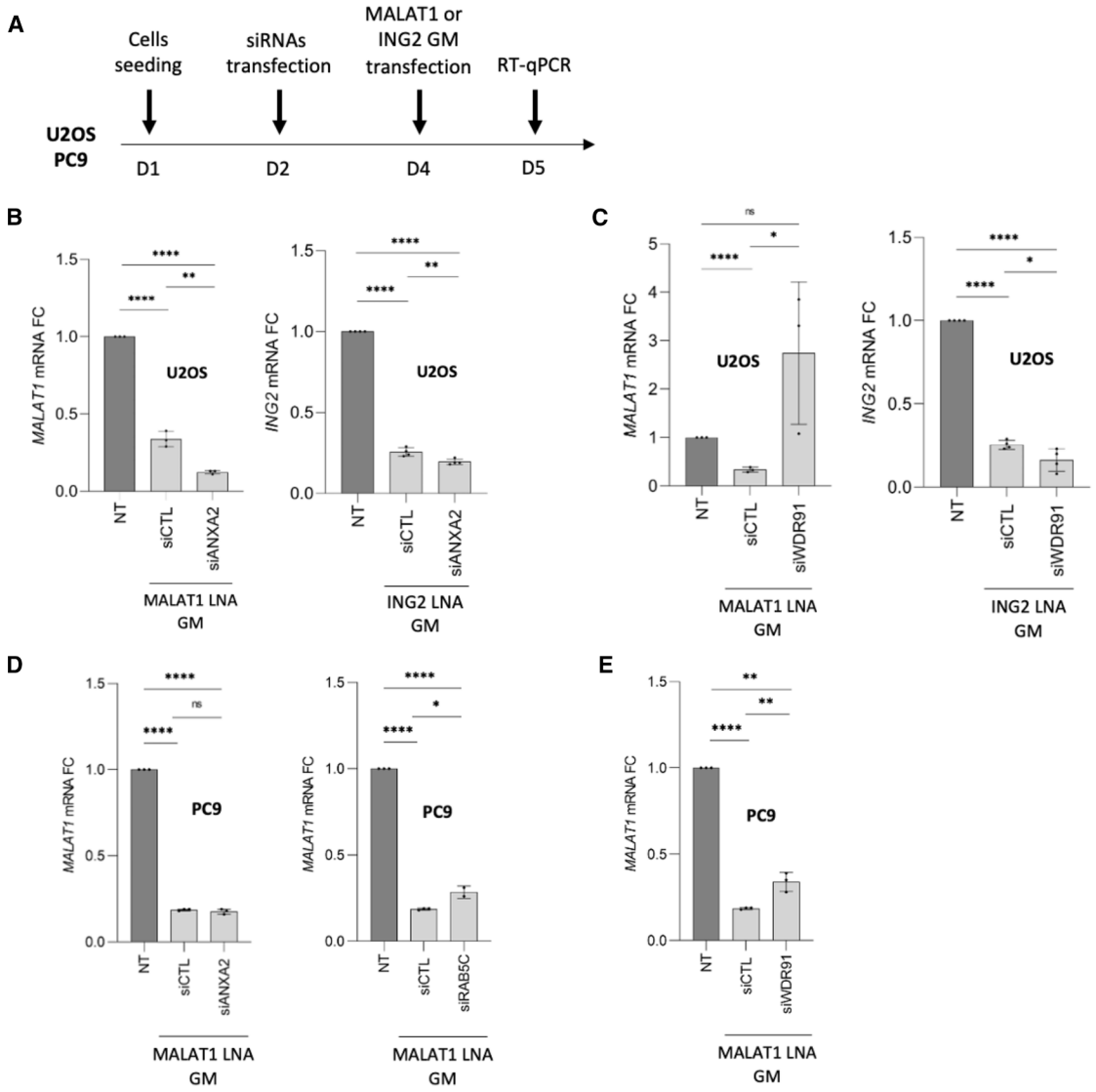

Figure 6. Functional validation of WDR91 in U2OS and PC9 cells

(A) Workflow of the experimental design, (B) *MALAT1* and *ING2* mRNA quantification by RT-qPCR at D5, after corresponding GM transfection on non-treated (NT), control, or ANXA2 knockdown U2OS cells. The relative mRNA FC was normalized to the NT condition (no siRNA transfection). Experiments were performed in independent biological replicates. Data are presented as mean (SD). Unpaired *t* test were performed. The statistical significance is ****$p < 0.0001$ (NT vs. siCTL; NT vs. siANXA2 – ING2); ****$p < 0.0001$ (NT vs. siCTL; NT vs. siANXA2 – MALAT1); **$p = 0.0020$ (siCTL vs. siANXA2 – MALAT1); **$p = 0.0090$ (siCTL vs. siANXA2 – ING2). (C) *MALAT1* and *ING2* mRNA quantification by RT-qPCR at D5, after corresponding GM transfection on NT, control or WDR91 knockdown U2OS cells. The relative mRNA FC was normalized to the NT condition (no siRNA transfection). Experiments were performed in independent biological replicates. Data are presented as mean (SD). Unpaired *t* test were performed. The statistical significance is ****$p < 0.0001$ (NT vs. siCTL – MALAT1); *$p = 0.0468$ (siCTL vs. siWDR91 – MALAT1); ****$p < 0.0001$ (NT vs. siCTL; NT vs. siWDR91 – ING2); *$p = 0.0415$ (siCTL vs. siWDR91 – ING2); NS = non-significant ($p = 0.1084$). (D) *MALAT1* mRNA quantification by RT-qPCR at D5, after corresponding GM transfection on NT, control, ANXA2, or RAB5C knockdown PC9 cells. The relative mRNA FC was normalized to the NT condition (no siRNA transfection). Experiments were performed in independent biological replicates. Data are presented as mean (SD). Unpaired *t* test were performed. The statistical significance is ****$p < 0.0001$ (NT vs. siCTL; NT vs. siANXA2 NT vs. siRAB5C); *$p = 0.0143$ (siCTL vs. siRAB5C); NS = non-significant ($p = 0.3486$). (E) *MALAT1* mRNA quantification by RT-qPCR at D5, after corresponding GM transfection on NT, control or WDR91 knockdown PC9 cells. The relative mRNA FC was normalized to the NT condition (no siRNA transfection). Experiments were performed in independent biological replicates. Data are presented as mean (SD). Unpaired *t* test were performed. The statistical significance is ****$p < 0.0001$ (NT vs. siCTL); **$p = 0.009$ (siCTL vs. siWDR91; NT vs. siWDR91).

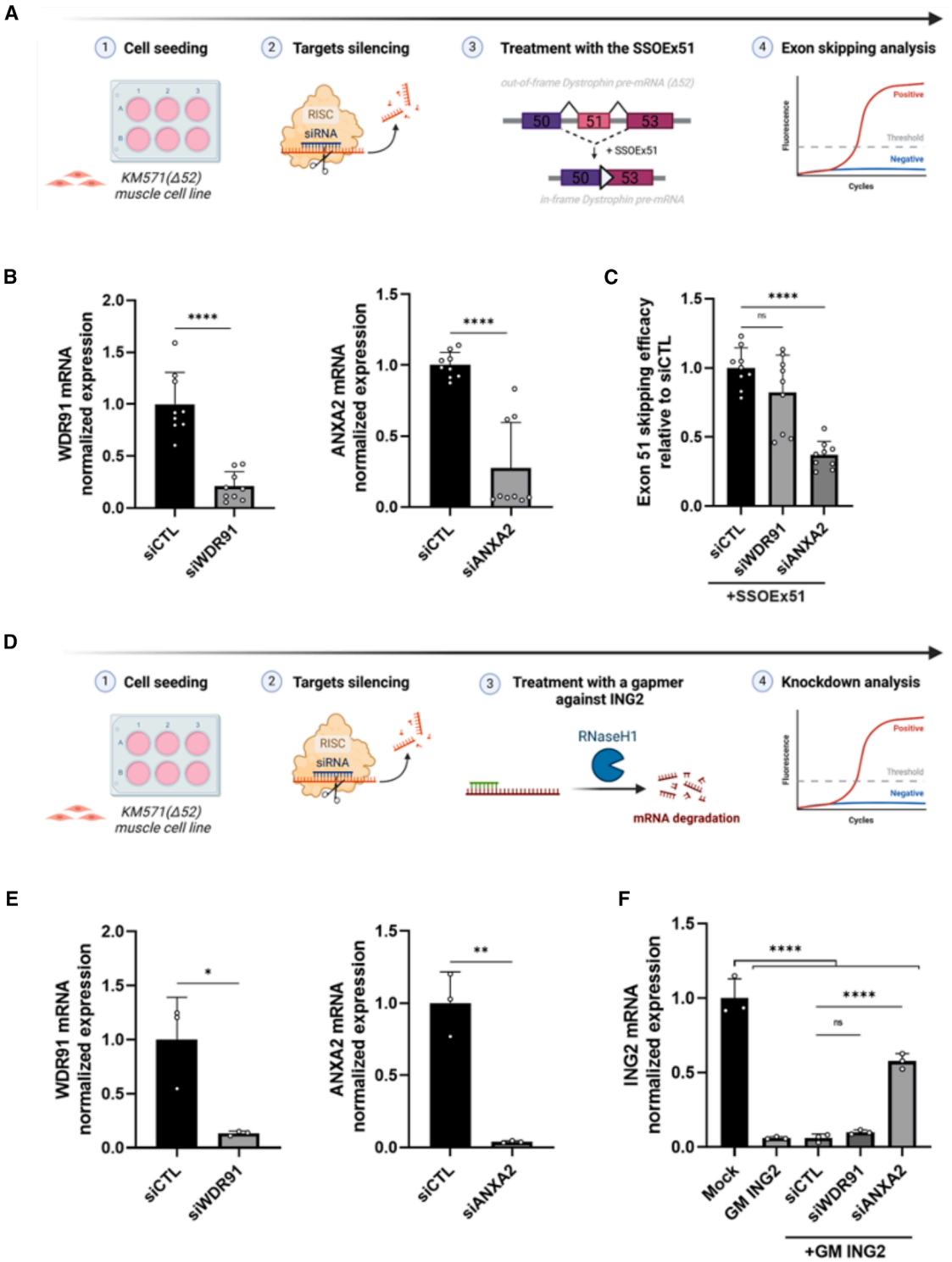

Figure 7. Functional validation of WDR91 in an immortalized DMD muscle cell line KM571

(A) Experimental setup for the double transfection protocol of siRNAs and SSOs in KM571 (B) *WDR91* and *ANXA2* mRNAs silencing efficiency. (C) *WDR91* and *ANXA2* mRNAs silencing effects on exon 51 skipping efficiency of the SSOEx51. (D) Experimental setup for the double transfection protocol of siRNAs and a GM

(legend continued on next page)

intracellular membranes and organelles. Moreover, the miRNA displacement mediated by a TSB ASO represents a relevant assay to investigate the proteins involved in ASOs efficiency, which has previously been validated *in vivo*.

This study revealed a set of 95 potential activators and 55 inhibitors. Among the activators, our assay highlighted the RAB5C and COG8 proteins, which are known positive regulators of ASOs trafficking and productive activity.[29,33] ANXA2, which is another known positive regulator, was not found in the list of candidates after application of our filters, which also shows that this type of CRISPR screen can be subject to false negatives.

Although ANXA2 is a well-characterized enhancer of ASOs activity, its downregulation in U2OS and PC9 cell lines did not impact the activity of MALAT1 and ING2 GMs. This suggest that ANXA2 may have an ASO-promoting activity that is cell line dependent. Indeed, it is known that identified proteins involved in ASO trafficking and productive activity might not have the same impact depending on the cell line (probably due to differences in high isoform co-expression or the establishment of compensatory proteins or pathways). The same observation was made, for example, in a study evaluating RAB5C, a well-characterized modulator of ASO activity.[46]

Of note, we observed that ANXA2 downregulation in U2OS cells enhanced the GM efficacy against MALAT1 and ING2. This was a surprising result as ANXA2 protein is an activator of ASOs activity. However, this result was not corroborated in PC9 cells, suggesting an experimental artifact or that U2OS might be an unstable model. Given the negative results regarding our ANXA2-positive control, we decided to include RAB5C as a new positive control. RAB5C knockdown significantly impaired the activity of MALAT1 GM in the PC9 cell line, further validating our loss-of-function assay.

In this study, we focused on WDR91 protein as a candidate of interest. This protein has a strong biological relevance as it is known to participate in the early-to-late endosome conversion and its knockdown showed the most significant inhibition of tcT3 anti-proliferative activity in our validation experiments.

We confirmed that WDR91 was a positive modulator of PS-ASO activity in two different assays (cell density assay and mRNA knockdown performance), with different cell models (501Mel, U2OS, and PC9) and ASO chemistries (tcDNA TSB and LNA GM), a landmark result of this project. However, the impact of WDR91 was not validated in all the systems studied. Indeed, WDR91 knockdown significantly impaired MALAT1 but not ING2 GM in U2OS cells. We found that *ING2* mRNA levels in non-treated cells were significantly higher compared with *MALAT1* mRNA levels, suggesting that, within our experimental setup, the effect of WDR91 knockdown could be dependent on the expression of the target RNA. In addition, WDR91 did not have any effect with a splice-switching ASOs in muscle cells. Thus, as is the case for ANXA2, WDR91 may have an ASO-promoting activity that is also cell type dependent.

Ultimately, the results of our validation experiments on various cell systems and ASO chemistries underline the need for caution when identifying an ASO modulator in a specific context, as it may not be applicable to all systems.

Productive PS-ASO release in the cytosol may occur mainly from late endosomes and MVBs,[24] as well as during the endosomal maturation process.[33] Interestingly, other studies have highlighted WDR91 as an important mediator of the release and efficacy of internalized reoviruses or antibody-drug conjugates in cells during the early endosome maturation or from the late endosomes.[30,47] We thus hypothesize that WDR91 may facilitate PS-ASO endosomal release during this endosomal maturation or from late endosomes and thus, participates in the global PS-ASO accumulation and activity in the cytosol and/or the nucleus.

Therefore, this study tends to further reinforce the key role of endosomal proteins in productive ASO trafficking and activity.

One of the limitations of our study is that genome-wide CRISPR screening was performed in a single replicate. Rigorous filters were used to identify robust ASO activity modulators. We have chosen to focus on a few selected proteins that promote internalized ASO activity, but it would also be interesting to validate other identified proteins as well as the potential inhibitors to confirm other candidates in 501Mel cells, as well as in other melanoma cell lines with different states of cell differentiation. Furthermore, and given the specificity of this cell type with regard to melanosome biogenesis and transport, involving numerous traffic processes,[48] it would be of interest to further evaluate WDR91 in other cell lines as it has been done in U2OS, PC9, and KM571 cells.

Analysis of the gene set enrichment also suggested new avenues to explore. Looking at the inhibitory proteins, some of them were associated with the endosomal cellular compartment. ATP6V0D2, for example, is one of the strongest inhibitor candidates in our selection and is involved in the acidification and pH maintenance in certain intracellular compartments.[49] Some activator candidates might be related to actin cytoskeleton regulation. From the related proteins, CDC42 and MAP2 are known to be involved in cellular trafficking disorders.[50] It is therefore relevant to consider that a defect in these

against ING2 (GM ING2) in KM571. (E) *WDR91* and *ANXA2* mRNAs silencing efficiency. (F) *WDR91* and *ANXA2* mRNAs silencing effects on ING2 knockdown induced by the GM ING2. Results are shown as the average of at least three independent biological replicates. Data are presented as mean (SD). The relative mRNA FC was normalized to the appropriate control condition (Mock or siCTL). Unpaired *t* test were performed. The statistical significance is $^{**}p < 0.005$; $^{****}p < 0.00005$; NS = non-significant.

proteins could also have an impact on intracellular trafficking and ASO release in melanoma.

Ultimately, our results contribute to a better characterization and identification of protein modulators of ASO activity, providing valuable information for potential new therapeutic avenue. Potent ASO modulators validated *in vitro* could be inhibited or overexpressed in *in vivo* experiments to assess and confirm an increase in ASO potency. Acting at the level of these modulators or directly on ASO-modulator interaction could result in more productive ASO activity, triggering an exacerbated inhibitory effect and an overall increase in the therapeutic index. Using the CRISPR tool is a method of choice for characterizing proteins involved in the trafficking, release, and productive activity of PS-ASOs. This method has recently been used to reveal AP1M1 role in ASO trafficking.[51]

MATERIALS AND METHODS

Cell lines and lentiviral library

501Mel, PC9, and U2OS cells were acquired from American Type Culture Collection. Before experiments, all cells were regularly tested for absence of mycoplasma. Culture and sub-culturing were performed in RPMI-1640 (Gibco) for 501Mel and PC9 and Mc Coy's 5A (Gibco) for U2OS, supplemented with 10% fetal bovine serum (Gibco), 2 mM L-glutamine (Gibco), and 1% penicillin/streptomycin (Gibco), and cultured at 37°C in a humidified incubator with 5% CO_2. Transfections and infections were performed in the same media but without antibiotics and with a decomplemented serum (30 min at 56°C). Immortalized myoblasts carrying a deletion of DMD exon 52 (KM571) were obtained from the platform for immortalization of human cells from the Institut de Myologie. KM571 cells were grown in a 50/50 mix of skeletal muscle cell growth medium (Promocell, Germany) and F-10 (Thermo Fisher Scientific) with 10% fetal bovine serum, and 1% penicillin-streptomycin (100 U/mL).

ASOs

miRCURY LNA TSBs TSB-C1 (ACTTTATTACAATCAT) and TSB-T3 (ACACAGTGGCAAACAC) were designed and obtained from Qiagen. tcC1 and tcT3 were synthesized from SQY Therapeutics (Montigny le Bretonneux) as fully modified tcDNA-PS ASOs. FAM-labelled LNA TSB-T3 ASO was designed and obtained from Qiagen. The TSB-C1 and tcC1 controls have no significant match to any annotated human 3′UTR. MALAT1 (CGTTAACTAGGCTTTA) and ING2 (TACGTTGGCTTGTTCA) LNA GMs were designed and obtained from Qiagen. For the KM571 experiments, all ASOs were obtained from Eurogentec. Three chemistries of the SSO targeting exon 51 (SSOEx51 previously described)[52] were used: LNA/2′MOE PS mixmer, full 2′MOE PS, and full tcDNA-PS. MALAT1 GM is a 2′MOE PS (previously described).[34] All ASOs were reconstituted in nuclease-free water (Invitrogen). All ASOs sequences are detailed in Table S3.

siRNAs

siRNAs pools were purchased from Santa Cruz (negative control A sc-37007; WDR91 sc-89398; WBSCR16 sc-89899; FH sc-105377; ELMOD1 sc-77261; TADA2B sc-156169; and ANXA2 sc-270151).

Generation of 501Mel knockout library

Transduction of mycoplasma negative 501Mel cells at 60% confluence was performed in T175 flasks (standard; Sarstedt) with the Brunello knockout pooled lentiviral library from Addgene (# 73179-LV) and in RPMI-1640 decomplemented medium (Gibco) without antibiotics. The Brunello pooled lentiviral library contains 76,441 sgRNAs, targeting 19,114 coding genes (4 sgRNAs per gene). A MOI of 0.4 was selected to ensure that every single cell is infected with only one sgRNA. Twenty-four hours later, the infectious medium was replaced by a fresh complete medium. After 48 h, infected cells were positively selected with 2.5 μg/mL puromycin (InvivoGen) for 7 days. Following selection and expansion of the surviving cells, approximately 350 million cells were recovered. A dry pellet of 100 million cells was prepared for gDNA extraction and sequencing. The remaining cells were used for the subsequent reverse transfection.

RNA interference, ASO treatments, and cell density assay

501Mel parental cells

Reverse-transfections of siRNAs were performed in 60-mm dishes (standard; Sarstedt) with 224,000 cells per dish and for 48 h in RPMI-1640 decomplemented medium without antibiotics. Briefly, 1-mL lipoplexes layers were formed with Lipofectamine 2000 (Invitrogen) and the siRNA concentrations were set to 30 nM in a final 3-mL volume after addition of the cells on top of the lipoplexes. For all the transfections, lipoplexes were formed in OptiMEM. After 16 h incubation, the medium was replaced by a fresh complete medium without antibiotics. After 48 h, cells were recovered, counted with a Neubauer counting chamber and a second reverse-transfection was performed in 96-well plates (standard F- Sarstedt) with 3000 cells per well and with either the siRNA alone (at 30 nM final concentration) or a combination of siRNA (30 nM) and tcT3 or LNA T3 at a final concentration of 50 nM in a final volume of 150 μL (100 μL of cells on top of 50 μL of lipoplexes). After 16 h incubation, the medium was replaced by a fresh 150-μL complete medium without antibiotics. After 4 days following to the second transfection, the cell density was measured with 0.5% crystal violet (10 min at room temperature, followed by three PBS washes, 100 μL of 100% EtOH solubilization, and absorbance reading at 590 nm using a Tecan Infinite F200 Pro reader).

U2OS and PC9 cells

Reverse-transfections of siRNAs were performed in 12-well plates (standard; Sarstedt) with 50,000 cells per well and for 48 h in decomplemented medium without antibiotics. Cell density was optimized so these cells are efficiently transfected between 20% and 30% confluence. The procedure was the same as described above except that the siRNA transfection was performed with RNAiMax (Invitrogen). After 48 h, the medium was replaced a reverse transfection with RNAiMax was performed in the same plate with the MALAT1 or ING2 GM (at 30 nM final concentration) in a final volume of 0.8mL (0.4 mL of lipoplexes on top of the cells). After 24 h following to the second transfection, total RNA was extracted for further RT-qPCR analysis.

501Mel knockout library

Reverse transfections of tcT3 and C1 were performed in 150-mm dishes (standard; Sarstedt) with 1.5 million knockout cells per dish and for 72 h in RPMI-1640 decomplemented medium without antibiotics. Briefly, 10-mL lipoplexes layers were formed with Lipofectamine 2000 (Invitrogen) and the respective ASOs concentrations were set to 50 nM in a final 24-mL volume after addition of the cells on top of the lipoplexes. For the transfections, lipoplexes were formed in OptiMEM and the mycoplasma-negative knockout cells have been sub-cultured 24 h before in T175 flasks (standard; Sarstedt). The cells confluency at the day of transfection was maintained between 50% and 80%. After 7 h of transfection, the medium was replaced by a fresh complete medium without antibiotics. To ensure a coverage of 400 cells per guide RNA in our library, a total of 32 million cells was transfected with either the tcT3 or C1. Thus, 22 dishes were used per oligonucleotide transfection. After 72 h of transfection, surviving cells were recovered and pellets of 100 million cells were kept at −80°C until further processing.

KM571 cells

Cells were plated in six-well plates (300,000 cells per well) and transfected the same day with 20 nM of siRNA with Lipofectamine RNAiMAX according to the manufacturer's instructions (Thermo Fisher Scientific). Twenty-four hours after the first transfection, proliferation medium was changed for differentiation medium (DMEM, 2% horse serum, 1% penicillin/streptomycin [100 U/mL]) to induce myotubes formation. After 3 days of differentiation, cells were treated with 100 nM of the SSOEx51 or SSOEx53 for 24 h with Lipofectamine LTX according to the manufacturer's instructions (Thermo Fisher Scientific). For the transfection of the GM ING2, similar protocol was used, except that KM571 cells were treated with 50 nM of the GM ING2.

NGS sequencing library preparation

Frozen pellets of 100 million transfected surviving cells (and from non-treated knockout library) in 50-mL poplypropylene tubes (Sarstedt) were thawed on ice for 20 min and lysed at room temperature. gDNA was purified according to the manufacturer's instructions (NucleoBond HMW DNA, Macherey-Nagel). A total of 280 μg of gDNAs was used for PCR amplification of sgRNA sequences, using the Herculase II Fusion polymerase (Agilent). Illumina P5- and P7-barcoded adaptors were used, and PCR amplification and quality controls have been carried out as described by Zhang laboratory (Joung et al., 2017). Amplified PCR products were purified using AMPure XP beads (Beckman Coulter) according to the manufacturer's instructions, eluted in 14 μL of nuclease-free water (Invitrogen) and stored at −20°C until Bioanalyzer quality control (TapeStation 4200, Agilent) was used to measure the size, quality and concentration. The pooled samples were sequenced using Illumina NGS sequencing platform (Novaseq6000, CurieCoreTech ICGex Platform).

NGS data analysis

MAGeCK (v0.5.9.4) was used to extract sgRNA read counts from the samples fastq.gz files (mageck count program with the –norm-method median option). For each sgRNA, we transformed the read counts onto M (log ratio) and A (mean average): M = log2 (sgRNA_count_in_TRT + 1) − log2(sgRNA_count_in_CTL + 1), and A = mean (count_TRT, count_CTL) in log2 scale. Fold-changes between TRT and CTL conditions were also computed from the M values of each sgRNA. All sgRNAs names and sequences are detailed in Table S4.

RNA extraction and RT-qPCR analysis

Total RNA form cell lysates was obtained using a NucleoSpin RNA kit (Macherey-Nagel), according to the manufacturer's instructions and with on-column DNAse treatment. After Nanodrop evaluation of purity and concentration, 500 ng of RNA was used for reverse-transcription (MultiScribe RT; Applied Biosystems). Obtained cDNA was diluted to 2.5 ng/μL and used as template for qPCR using a QuantStudio5 system (Applied Biosystems). SYBR Green (PowerSYBR Green PCR Master Mix; Applied Biosystems) was used according to the manufacturer's instructions. For each sample measurement, three technical replicates were performed. TBP was used as internal standard. TYRP1 and ING2 primers were purchased from Eurogentec. Percent knockdown was calculated as $100 \times (1 - 2^{-\mathrm{ddCt}})$. Total RNA was isolated from cultured human myoblast cells using TRIzol reagent, according to the manufacturer's instructions (Thermo Fisher Scientific). Aliquots of 1 μg of total RNA were used for RT-PCR analysis. The cDNA synthesis was carried out with LunaScript RT SuperMix Kit (New England Biolabs). Exon 51 skipping was measured by TaqMan qRT-PCR, using TaqMan assays that were designed against the exon 51–53 or exon 50–53 templates using the Prime Time qPCR probe assays (Integrated DNA Technology) (Assay Ex51–53—forward: 5′-CAGGTTGTGTCACCAGAG TAA-3′; reverse 5′-TGAGTGGAAGGCGGTAAA-3′; probe: 5′-/56-FAM/TGACCACTA/ZEN/TTGGAGCCTCTCCTAC/3IABkFQ/-3′ and assay Ex50–53: forward: 5′-ACTGATTCTGAATTCTTTCAAA GGC-3′; reverse: 5′-TTCAAGAGCTGAGGGCAAAG-3′; probe: 5′-/56-FAM/ACCTAGCTC/ZEN/CTGGACTGACCACT/3IABkFQ/-3′). gBlocks Gene Fragments (Integrated DNA Technology) from human exon 49–54 and human exon 49–54 Delta 52 were used as standards for DNA copy number. We used 70 ng of cDNA as input per reaction, and all assays were carried out in triplicate. Assays were performed under fast cycling conditions on a Bio-Rad CFX384 Touch Real-Time PCR Detection System. For a given sample, the copy number of skipped product (exon 50–53 assay) and unskipped product (exon 51–53 assay) was determined using the standards Ex49-54 and Ex49-54 Delta52, respectively. Exon 51 skipping was then expressed as a percentage of total dystrophin. For exon 53 skipping, similar procedure was used with the appropriate assay design (preexisting assay Ex53-54 from Integrated DNA Technologies [IDT]: Hs.PT.58.24504618.g and assay Ex51-54 - forward: 5′-GAACTTACCGACTGGCTTTCT-3′; reverse 5′-TCTTTGGCC AACTGCTTCT-3′; probe: 5′-/56-FAM/AAATCACAG/ZEN/AGG GTGATGGTGGGT/3IABkFQ/-3′). gBlocks Gene Fragments (Integrated DNA Technology) from human exon 49–54 and human exon 49–54 Delta 53 were used as standards for DNA copy number in these experiments. Knockdown analysis was performed by

using the appropriate primers for the studied targets and were purchased from IDT (MALAT1 Hs.PT.58.26451167.g; WDR91 Hs.PT.58.39523053, and ANXA2 Hs.PT.56a.40676274) or provided by Eurogentec for ING2. The expression of the different targets was then normalized to a reference gene (GAPDH Hs.PT.39a.22214836).

Protein isolation and western blotting

Total protein extracts were obtained by resuspension of PBS-washed cell pellets in 40µL of ice-cold RIPA buffer (Tris-HCl 50 mM, pH 7.4, NaCl 150 mM, sodium deoxycholate 0.5%, Triton 1%, SDS 0.1%), including protease inhibitor cocktail (Sigma-Aldrich, P8340) and centrifugation at 16,000×*g* for 15 min at 4°C. Proteins quantification from the cleared lysates was performed using a Pierce BCA Assay kit (Thermo Risher Scientific). After 4%–12% SDS-PAGE in NuPAGE MES buffer (Invitrogen), proteins were transferred onto PVDF membranes with a turbo transfer system (BIO-RAD) for 10 min at 25 V and 2.5 A. After transfer, the membranes were washed in Tris-buffered saline and 0.1% Tween 20 (TBST) and blocked for 30 min at room temperature in a solution of TBST +5% w/v non-fat dry milk. Blocked membranes were washed three times in TBST for 5 min and diluted primary antibody was incubated at 4°C overnight with shaking. The diluted horseradish peroxidase-conjugated secondary antibody was added for 1 h at room temperature with shaking, after three TBST washes of 5 min. Imaging was performed after ECL reagent addition and chemiluminescence detection with G:Box Chemi XX6 imager from Syngene. ANXA2 antibody was purchased from Santa Cruz (sc-28385). WDR91 antibody was purchased from biotechne (NB100-77307).

Confocal microscopy

501Mel cells were reverse transfected for 48 h in 60-mm dishes (standard; Sarstedt) with either a control siRNA or a WDR91-targeted siRNA at a final concentration of 30 nM in a final volume of 3 mL (2 mL of cells on top of 1 mL of lipoplexes). Then, the cells were recovered, counted with a Neubauer counting chamber and a second reverse transfection was performed in chamber slides (Labtek) with 25,000 cells per chamber and with a FAM-labelled ASO (at 50 nM final concentration) in a final volume of 1 mL (800 µL of cells on top of 200 µL of lipoplexes). After incubation for 8 h, cells were stained with Hoechst 33258 (Sigma-Aldrich) for 15 min at room temperature and washed twice with PBS. After washing, the cells were fixed in 4% formaldehyde for 20 min at room temperature and washed twice with PBS. Cells were mounted and observed under a confocal microscope (Leica SP8). Confocal images were analyzed by Fiji software.

Statistical analysis

GraphPad Prism software (San Diego, CA) version 9.5.1 was used for statistical analysis and graphs design. Each data is presented as mean of at least three independent biological replicates with SD. *p* values were calculated by two-sided unpaired *t* tests and differences were statistically significant at $^{*}p \leq 0.05$; $^{**}p \leq 0.01$; $^{***}p \leq 0.001$; $^{****}p \leq 0.0001$. For exon skipping experiments, normal distribution of samples was assessed by using the Shapiro-Wilk test. Comparisons of statistical significance were assessed by one-way ANOVA parametric test or Kruskal-Wallis non-parametric test and followed by appropriate *post hoc* tests if applicable.

DATA AVAILABILITY

Data are available upon request to the corresponding author.

ACKNOWLEDGMENTS

The authors thank the L3 and MRic platforms of Rennes University (UMS BIOSIT, UAR3480 CNRS US18 INSERM) for providing the required facilities for performing the lentiviral infections and the confocal microscopy. The authors also thank the Institut Curie (Genetic screen CRISPR'it and ICGex Core Facilities) for performing the NGS sequencing, SQY Therapeutics for providing the tcDNA-ASO molecules and the platform for the immortalization of human cells from the Institut de Myologie for the human-derived cells. This study received financial support from the Agence Nationale de la Recherche (ANR-21-CE18-0020).

AUTHOR CONTRIBUTIONS

G.M., R.P., D.G., A. Goyenvalle, and A. Gaci. conceived and analyzed the experiments. G.M. and A. Gaci performed the experiments. M.A. analyzed the NGS raw data. A.M. and A.B. helped in the library preparation. G.M. wrote the manuscript. All the authors reviewed the manuscript.

DECLARATION OF INTERESTS

The authors declare no competing interests.

SUPPLEMENTAL INFORMATION

Supplemental information can be found online at https://doi.org/10.1016/j.omtn.2025.102577.

REFERENCES

1. Crooke, S.T., Liang, X.-H., Baker, B.F., and Crooke, R.M. (2021). Antisense Technology: A Review. J. Biol. Chem. *296*, 100416. https://doi.org/10.1016/j.jbc.2021.100416.

2. Kim, J., Hu, C., Moufawad El Achkar, C., Black, L.E., Douville, J., Larson, A., Pendergast, M.K., Goldkind, S.F., Lee, E.A., Kuniholm, A., et al. (2019). Patient-Customized Oligonucleotide Therapy for a Rare Genetic Disease. N. Engl. J. Med. *381*, 1644–1652. https://doi.org/10.1056/NEJMoa1813279.

3. Crooke, S.T., Wang, S., Vickers, T.A., Shen, W., and Liang, X.-H. (2017). Cellular Uptake and Trafficking of Antisense Oligonucleotides. Nat. Biotechnol. *35*, 230–237. https://doi.org/10.1038/nbt.3779.

4. Xie, X., Yu, T., Li, X., Zhang, N., Foster, L.J., Peng, C., Huang, W., and He, G. (2023). Recent Advances in Targeting the 'Undruggable' Proteins: From Drug Discovery to Clinical Trials. Signal Transduct. Targeted Ther. *8*, 335–371. https://doi.org/10.1038/s41392-023-01589-z.

5. Egli, M., and Manoharan, M. (2023). Chemistry, Structure and Function of Approved Oligonucleotide Therapeutics. Nucleic Acids Res. *51*, 2529–2573. https://doi.org/10.1093/nar/gkad067.

6. Nie, T. (2024). Eplontersen: First Approval. Drugs (Basel) *84*, 473–478. https://doi.org/10.1007/s40265-024-02008-5.

7. Xiong, H., Veedu, R.N., and Diermeier, S.D. (2021). Recent Advances in Oligonucleotide Therapeutics in Oncology. Int. J. Mol. Sci. *22*, 3295. https://doi.org/10.3390/ijms22073295.

8. Gagliardi, M., and Ashizawa, A.T. (2021). The Challenges and Strategies of Antisense Oligonucleotide Drug Delivery. Biomedicines *9*, 433. https://doi.org/10.3390/biomedicines9040433.

9. Hammond, S.M., Aartsma-Rus, A., Alves, S., Borgos, S.E., Buijsen, R.A.M., Collin, R.W.J., Covello, G., Denti, M.A., Desviat, L.R., Echevarría, L., et al. (2021). Delivery of Oligonucleotide-based Therapeutics: Challenges and Opportunities. EMBO Mol. Med. *13*, e13243. https://doi.org/10.15252/emmm.202013243.

10. Juliano, R.L., Ming, X., Carver, K., and Laing, B. (2014). Cellular Uptake and Intracellular Trafficking of Oligonucleotides: Implications for Oligonucleotide Pharmacology. Nucleic Acid Therapeut. *24*, 101–113. https://doi.org/10.1089/nat.2013.0463.

11. Klipp, A., Burger, M., and Leroux, J.-C. (2023). Get out or Die Trying: Peptide- and Protein-Based Endosomal Escape of RNA Therapeutics. Adv. Drug Deliv. Rev. *200*, 115047. https://doi.org/10.1016/j.addr.2023.115047.

12. Dowdy, S.F., Setten, R.L., Cui, X.-S., and Jadhav, S.G. (2022). Delivery of RNA Therapeutics: The Great Endosomal Escape. Nucleic Acid Therapeut. *32*, 361–368. https://doi.org/10.1089/nat.2022.0004.

13. Aupy, P., Echevarría, L., Relizani, K., and Goyenvalle, A. (2017). The Use of Tricyclo-DNA Oligomers for the Treatment of Genetic Disorders. Biomedicines *6*, 2. https://doi.org/10.3390/biomedicines6010002.

14. Godfrey, C., Desviat, L.R., Smedsrød, B., Piétri-Rouxel, F., Denti, M.A., Disterer, P., Lorain, S., Nogales-Gadea, G., Sardone, V., Anwar, R., et al. (2017). Delivery Is Key: Lessons Learnt from Developing Splice-switching Antisense Therapies. EMBO Mol. Med. *9*, 545–557. https://doi.org/10.15252/emmm.201607199.

15. Alhamadani, F., Zhang, K., Parikh, R., Wu, H., Rasmussen, T.P., Bahal, R., Zhong, X.-B., and Manautou, J.E. (2022). Adverse Drug Reactions and Toxicity of the Food and Drug Administration-Approved Antisense Oligonucleotide Drugs. Drug Metab. Dispos. *50*, 879–887. https://doi.org/10.1124/dmd.121.000418.

16. Liang, X.-H., Sun, H., Shen, W., and Crooke, S.T. (2015). Identification and Characterization of Intracellular Proteins That Bind Oligonucleotides with Phosphorothioate Linkages. Nucleic Acids Res. *43*, 2927–2945. https://doi.org/10.1093/nar/gkv143.

17. Crooke, S.T., Seth, P.P., Vickers, T.A., and Liang, X.-H. (2020). The Interaction of Phosphorothioate-Containing RNA Targeted Drugs with Proteins Is a Critical Determinant of the Therapeutic Effects of These Agents. J. Am. Chem. Soc. *142*, 14754–14771. https://doi.org/10.1021/jacs.0c04928.

18. Liang, X.-H., Shen, W., Sun, H., Kinberger, G.A., Prakash, T.P., Nichols, J.G., and Crooke, S.T. (2016). Hsp90 Protein Interacts with Phosphorothioate Oligonucleotides Containing Hydrophobic 2′-Modifications and Enhances Antisense Activity. Nucleic Acids Res. *44*, 3892–3907. https://doi.org/10.1093/nar/gkw144.

19. Miller, C.M., Donner, A.J., Blank, E.E., Egger, A.W., Kellar, B.M., Østergaard, M.E., Seth, P.P., and Harris, E.N. (2016). Stabilin-1 and Stabilin-2 Are Specific Receptors for the Cellular Internalization of Phosphorothioate-Modified Antisense Oligonucleotides (ASOs) in the Liver. Nucleic Acids Res. *44*, 2782–2794. https://doi.org/10.1093/nar/gkw112.

20. Van de Vyver, T., De Smedt, S.C., and Raemdonck, K. (2022). Modulating Intracellular Pathways to Improve Non-Viral Delivery of RNA Therapeutics. Adv. Drug Deliv. Rev. *181*, 114041. https://doi.org/10.1016/j.addr.2021.114041.

21. Finicle, B.T., Eckenstein, K.H., Revenko, A.S., Anderson, B.A., Wan, W.B., McCracken, A.N., Gil, D., Fruman, D.A., Hanessian, S., Seth, P.P., and Edinger, A.L. (2023). Simultaneous Inhibition of Endocytic Recycling and Lysosomal Fusion Sensitizes Cells and Tissues to Oligonucleotide Therapeutics. Nucleic Acids Res. *51*, 1583–1599. https://doi.org/10.1093/nar/gkad023.

22. Kapustin, A.N., Davey, P., Longmire, D., Matthews, C., Linnane, E., Rustogi, N., Stavrou, M., Devine, P.W.A., Bond, N.J., Hanson, L., et al. (2021). Antisense Oligonucleotide Activity in Tumour Cells Is Influenced by Intracellular LBPA Distribution and Extracellular Vesicle Recycling. Commun. Biol. *4*, 1241. https://doi.org/10.1038/s42003-021-02772-0.

23. Wagenaar, T.R., Tolstykh, T., Shi, C., Jiang, L., Zhang, J., Li, Z., Yu, Q., Qu, H., Sun, F., Cao, H., et al. (2015). Identification of the Endosomal Sorting Complex Required for Transport-I (ESCRT-I) as an Important Modulator of Anti-miR Uptake by Cancer Cells. Nucleic Acids Res. *43*, 1204–1215. https://doi.org/10.1093/nar/gku1367.

24. Wang, S., Allen, N., Liang, X.-H., and Crooke, S.T. (2018). Membrane Destabilization Induced by Lipid Species Increases Activity of Phosphorothioate-Antisense Oligonucleotides. Mol. Ther. Nucleic Acids *13*, 686–698. https://doi.org/10.1016/j.omtn.2018.10.011.

25. Lorenz, P., Misteli, T., Baker, B.F., Bennett, C.F., and Spector, D.L. (2000). Nucleocytoplasmic Shuttling: A Novel in Vivo Property of Antisense Phosphorothioate Oligodeoxynucleotides. Nucleic Acids Res. *28*, 582–592.

26. Castanotto, D., Zhang, X., Alluin, J., Zhang, X., Rüger, J., Armstrong, B., Rossi, J., Riggs, A., and Stein, C.A. (2018). A Stress-Induced Response Complex (SIRC) Shuttles miRNAs, siRNAs, and Oligonucleotides to the Nucleus. Proc. Natl. Acad. Sci. USA *115*, E5756–E5765. https://doi.org/10.1073/pnas.1721346115.

27. Hanswillemenke, A., Hofacker, D.T., Sorgenfrei, M., Fruhner, C., Franz-Wachtel, M., Schwarzer, D., Maček, B., and Stafforst, T. (2024). Profiling the Interactome of Oligonucleotide Drugs by Proximity Biotinylation. Nat. Chem. Biol. *20*, 555–565. https://doi.org/10.1038/s41589-023-01530-z.

28. Bock, C., Datlinger, P., Chardon, F., Coelho, M.A., Dong, M.B., Lawson, K.A., Lu, T., Maroc, L., Norman, T.M., Song, B., et al. (2022). High-Content CRISPR Screening. Nat. Rev. Methods Primers *2*, 8–23. https://doi.org/10.1038/s43586-021-00093-4.

29. Petitjean, O., Girardi, E., Ngondo, R.P., Lupashin, V., and Pfeffer, S. (2020). Genome-Wide CRISPR-Cas9 Screen Reveals the Importance of the Heparan Sulfate Pathway and the Conserved Oligomeric Golgi Complex for Synthetic Double-Stranded RNA Uptake and Sindbis Virus Infection. mSphere *5*, e00914-20. https://doi.org/10.1128/mSphere.00914-20.

30. Tsui, C.K., Barfield, R.M., Fischer, C.R., Morgens, D.W., Li, A., Smith, B.A.H., Gray, M.A., Bertozzi, C.R., Rabuka, D., and Bassik, M.C. (2019). CRISPR-Cas9 Screens Identify Regulators of Antibody–Drug Conjugate Toxicity. Nat. Chem. Biol. *15*, 949–958. https://doi.org/10.1038/s41589-019-0342-2.

31. Ross-Thriepland, D., Bornot, A., Butler, L., Desai, A., Jaiswal, H., Peel, S., Hunter, M. R., Odunze, U., Isherwood, B., and Gianni, D. (2020). Arrayed CRISPR Screening Identifies Novel Targets That Enhance the Productive Delivery of mRNA by MC3-Based Lipid Nanoparticles. SLAS Discov. *25*, 605–617. https://doi.org/10.1177/2472555220925770.

32. McMahon, M.A., Rahdar, M., Mukhopadhyay, S., Bui, H.-H., Hart, C., Damle, S., Courtney, M., Baughn, M.W., Cleveland, D.W., and Bennett, C.F. (2023). GOLGA8 Increases Bulk Antisense Oligonucleotide Uptake and Activity in Mammalian Cells. Mol. Ther. Nucleic Acids *32*, 289–301. https://doi.org/10.1016/j.omtn.2023.03.017.

33. Miller, C.M., Wan, W.B., Seth, P.P., and Harris, E.N. (2018). Endosomal Escape of Antisense Oligonucleotides Internalized by Stabilin Receptors Is Regulated by Rab5C and EEA1 During Endosomal Maturation. Nucleic Acid Therapeut. *28*, 86–96. https://doi.org/10.1089/nat.2017.0694.

34. Wang, S., Sun, H., Tanowitz, M., Liang, X.-H., and Crooke, S.T. (2016). Annexin A2 Facilitates Endocytic Trafficking of Antisense Oligonucleotides. Nucleic Acids Res. *44*, 7314–7330. https://doi.org/10.1093/nar/gkw595.

35. Gilot, D., Migault, M., Bachelot, L., Journé, F., Rogiers, A., Donnou-Fournet, E., Mogha, A., Mouchet, N., Pinel-Marie, M.-L., Mari, B., et al. (2017). A Non-Coding Function of TYRP1 mRNA Promotes Melanoma Growth. Nat. Cell Biol. *19*, 1348–1357. https://doi.org/10.1038/ncb3623.

36. Gautron, A., Migault, M., Bachelot, L., Corre, S., Galibert, M.-D., and Gilot, D. (2021). Human TYRP1: Two Functions for a Single Gene? Pigment Cell Melanoma Res. *34*, 836–852. https://doi.org/10.1111/pcmr.12951.

37. Aupy, P., Echevarría, L., Relizani, K., Zarrouki, F., Haeberli, A., Komisarski, M., Tensorer, T., Jouvion, G., Svinartchouk, F., Garcia, L., et al. (2019). Identifying and Avoiding tcDNA-ASO Sequence-Specific Toxicity for the Development of DMD Exon 51 Skipping Therapy. Mol. Ther. Nucleic Acids *19*, 371–383. https://doi.org/10.1016/j.omtn.2019.11.020.

38. Imbert, M., Blandel, F., Leumann, C., Garcia, L., and Goyenvalle, A. (2019). Lowering Mutant Huntingtin Using Tricyclo-DNA Antisense Oligonucleotides As a Therapeutic Approach for Huntington's Disease. Nucleic Acid Therapeut. *29*, 256–265. https://doi.org/10.1089/nat.2018.0775.

39. Doench, J.G. (2018). Am I Ready for CRISPR? A User's Guide to Genetic Screens. Nat. Rev. Genet. *19*, 67–80. https://doi.org/10.1038/nrg.2017.97.

40. Sanson, K.R., Hanna, R.E., Hegde, M., Donovan, K.F., Strand, C., Sullender, M.E., Vaimberg, E.W., Goodale, A., Root, D.E., Piccioni, F., and Doench, J.G. (2018). Optimized Libraries for CRISPR-Cas9 Genetic Screens with Multiple Modalities. Nat. Commun. *9*, 5416. https://doi.org/10.1038/s41467-018-07901-8.

41. Hu, Y., Comjean, A., Attrill, H., Antonazzo, G., Thurmond, J., Li, F., Chao, T., Mohr, S.E., Brown, N.H., and Perrimon, N. (2023). PANGEA: A New Gene Set Enrichment Tool for Drosophila and Common Research Organisms. Preprint at bioRxiv. https://doi.org/10.1101/2023.02.20.529262.

42. Liu, K., Xing, R., Jian, Y., Gao, Z., Ma, X., Sun, X., Li, Y., Xu, M., Wang, X., Jing, Y., et al. (2017). WDR91 Is a Rab7 Effector Required for Neuronal Development. J. Cell Biol. *216*, 3307–3321. https://doi.org/10.1083/jcb.201705151.

43. Liu, N., Liu, K., and Yang, C. (2022). WDR91 Specifies the Endosomal Retrieval Subdomain for Retromer-Dependent Recycling. J. Cell Biol. *221*, e202203013. https://doi.org/10.1083/jcb.202203013.

44. Vickers, T.A., and Crooke, S.T. (2016). Development of a Quantitative BRET Affinity Assay for Nucleic Acid-Protein Interactions. PLoS One *11*, e0161930. https://doi.org/10.1371/journal.pone.0161930.

45. Goyenvalle, A., Griffith, G., Babbs, A., El Andaloussi, S., Ezzat, K., Avril, A., Dugovic, B., Chaussenot, R., Ferry, A., Voit, T., et al. (2015). Functional Correction in Mouse Models of Muscular Dystrophy Using Exon-Skipping Tricyclo-DNA Oligomers. Nat. Med. *21*, 270–275. https://doi.org/10.1038/nm.3765.

46. Linnane, E., Davey, P., Zhang, P., Puri, S., Edbrooke, M., Chiarparin, E., Revenko, A. S., Macleod, A.R., Norman, J.C., and Ross, S.J. (2019). Differential Uptake, Kinetics and Mechanisms of Intracellular Trafficking of next-Generation Antisense Oligonucleotides across Human Cancer Cell Lines. Nucleic Acids Res. *47*, 4375–4392. https://doi.org/10.1093/nar/gkz214.

47. Snyder, A.J., Abad, A.T., and Danthi, P. (2022). A CRISPR-Cas9 Screen Reveals a Role for WD Repeat-Containing Protein 81 (WDR81) in the Entry of Late Penetrating Viruses. PLoS Pathog. *18*, e1010398. https://doi.org/10.1371/journal.ppat.1010398.

48. Fukuda, M. (2021). Rab GTPases: Key Players in Melanosome Biogenesis, Transport, and Transfer. Pigment Cell Melanoma Res. *34*, 222–235. https://doi.org/10.1111/pcmr.12931.

49. Kissing, S., Hermsen, C., Repnik, U., Nesset, C.K., Von Bargen, K., Griffiths, G., Ichihara, A., Lee, B.S., Schwake, M., De Brabander, J., et al. (2015). Vacuolar ATPase in Phagosome-Lysosome Fusion. J. Biol. Chem. *290*, 14166–14180. https://doi.org/10.1074/jbc.M114.628891.

50. García-Cazorla, A., Oyarzábal, A., Saudubray, J.-M., Martinelli, D., and Dionisi-Vici, C. (2022). Genetic Disorders of Cellular Trafficking. Trends Genet. *38*, 724–751. https://doi.org/10.1016/j.tig.2022.02.012.

51. Malong, L., Roskosch, J., Hager, C., Fortin, J.-P., Schmucki, R., Callow, M.G., Weile, C., Romeo, V., Patsch, C., Martin, S., et al. (2024). A CRISPR/Cas9 screen reveals proteins at the endosome-Golgi interface that modulate cellular ASO activity. Preprint at bioRxiv. https://doi.org/10.1101/2024.12.17.628665.

52. Saoudi, A., Fergus, C., Gileadi, T., Montanaro, F., Morgan, J.E., Kelly, V.P., Tensorer, T., Garcia, L., Vaillend, C., Muntoni, F., and Goyenvalle, A. (2023). Investigating the Impact of Delivery Routes for Exon Skipping Therapies in the CNS of DMD Mouse Models. Cells *12*, 908. https://doi.org/10.3390/cells12060908.